Figure 24 shows the range distribution of π^+ and μ^+ from the more frequent K^+ decays at rest. A ± 1 cm range resolution is folded in. As can be seen from the figure, approximately 20% of the π^+ from $K^+ \to \pi^+\nu\bar{\nu}$ lie beyond the $\pi^+\pi^\circ$ peak. Thus unambiguous identification of π^+ with a range above that value would by itself constitute a signature of $K^+ \to \pi^+\nu\bar{\nu}$. Clearly the acceptance for $K^+ \to \pi^+ + f$ is complete in π^+ momentum space.

The experiment is also sensitive to other rare decay modes like $K^+ \to \pi^+e^+\mu^-$ (a $\Delta G = 2$ transition) and $K^+ \to \pi^+\gamma\gamma$. In addition, the decay $K^+ \to \pi^\circ\pi^+$ can be used as a source of tagged π°'s and provide a mechanism to search for $\pi^\circ \to$ nothing observed.

An ongoing parallel effort is an experiment[72] to measure the decay mode

$$K^+ \to \pi^+e^-\mu^+$$

down to a level of 10^{-11}, roughly a factor of 500 better than the existing present limit.[73] Experimentally, the advantage here lies in the fact that the initial and all final state particles are charged, facilitating the overall kinematic constraint of energy and momentum conservation. The main experimental challenge lies in the particle identification since the main background appears to be due to the reaction

$$K^+ \to \pi^+\pi^+\pi^-$$

followed by the $\pi^+ \to \mu^+\nu$ decay and misidentification of the π^- as an electron. Specifically a π^-/e^- rejection of 10^{-7} is required which is obtained by a pair of gas Čerenkov counters and a lead-scintillator shower detector. The plan view of the apparatus is shown in Fig. 25. The Čerenkov counter in the muon arm is used to suppress the background from the decay $K^+ \to \pi^+\pi^\circ$ with a subsequent decay $\pi^\circ \to e^+e^-\gamma$.

This experiment will also obtain several thousand of the examples of the decay $K^+ \to \pi^+e^+e^-$. This final state will allow one to search for states with mass

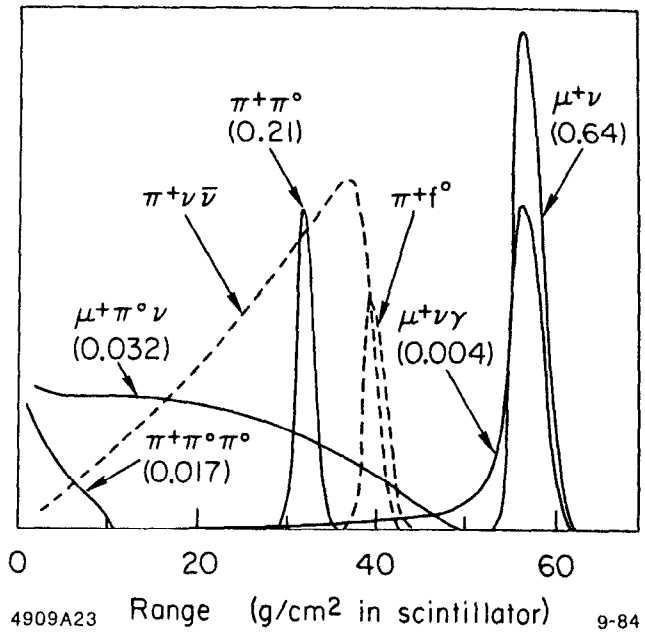

Figure 24 Range distribution in scintillator for π^+ and μ^+ from the known K^+ decays and from the rare decays searched for. The branching ratios of the known decays are indicated in parentheses.

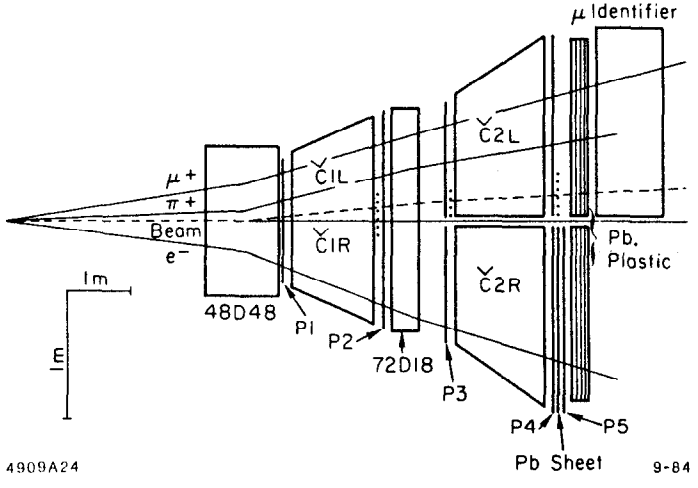

Figure 25 Plan view of the detection apparatus for the experiment searching for the decay mode $K^+ \to \pi^+\mu^+e^-$.

between 140 and 340 MeV decaying into e^+e^- and will provide an improvement of our knowledge of the branching ratio $\pi^\circ \to e^+e^-$.

The decay $K_L^\circ \to \mu^\pm e^\mp$ is being looked for by 2 experiments at BNL.[74,57] The decay $K_L^\circ \to \mu e$ is also a lepton number violating process but the same branching ratio sensitivity as in the $K^+ \to \pi\mu e$ decay translates into a limit on the strength of the interaction almost 2 orders of magnitude better. This is because of the longer K_L° lifetime and larger phase space for the 2 body final state. The main background comes from the relatively copious $K_L^\circ \to \pi e\nu$ decay followed by the $\pi \to \mu\nu$ decay. If the 2 ν's carry off minimum amounts of energy in the lab, this process can closely simulate the decay mode of interest. This background is especially pernicious if the $\pi \to \mu\nu$ decay occurs in the analyzing magnet since the decay kink in the right direction can increase the muon apparent momentum and thus allow the event to come even closer to faking the $K_L^\circ \to \mu e$ decay.

The schematic views of the Yale-BNL experiment are shown in Fig. 26. The electrons are identified by the Čerenkov counter and a lead glass wall (the particle identification is not extremely crucial in this experiment). Muon range is measured in an iron range stack to provide additional redundancy in μ energy measurement. Mini-drift chambers are used to obtain good position measurement, which is especially crucial in this kind of an experiment.

The Monte Carlo calculations indicate that the background begins to come in at a level of about 10^{-11}. The experiment is designed to achieve at least a 10^{-10} branching ratio sensitivity which would represent almost a two order of magnitude improvement over the present limit. In addition, a comparable sensitivity exists for the decay mode $K_L^\circ \to e^+e^-$. Since the standard model prediction for this decay is only about 10^{-13} (branching ratio) because of helicity suppression, new physics could manifest itself in that decay mode.

An even more ambitious proposal[57] has been put forth recently. It attempts to push this limit down to a branching ratio level of 10^{-12}. To achieve this, very high intensities are required (10^{13} protons/pulse) and one has to be able

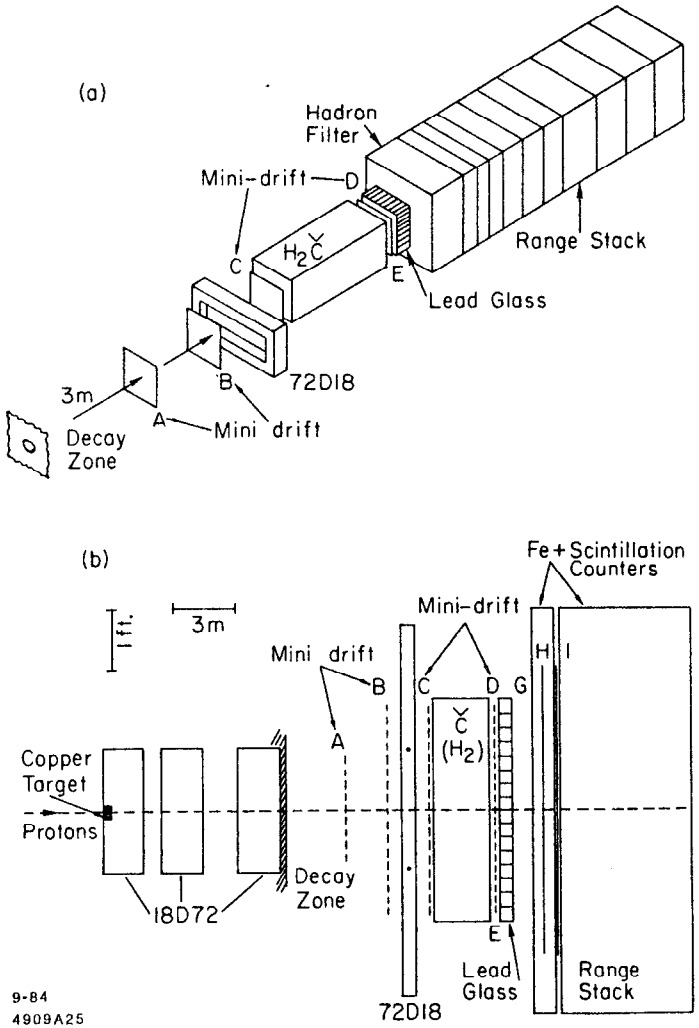

Figure 26 Schematic views, exploded (a) and plan (b) of the Yale-BNL detector used in E780.

to live in a flux of $6 \times 10^8 K_L^\circ$/pulse. The neutral beam has to be transported through the apparatus in a vacuum pipe, necessitating very good collimation upstream. To reduce the background below 10^{-12}, two independent spectrometers are used allowing one to perform two independent momentum measurements on both charged particles. In addition, the muon range stack is finely segmented to obtain an additional μ momentum measurement limited only by range straggling. The schematic of the proposed detector is shown in Fig. 27.

In addition to the comparable sensitivity for the decay mode $K_L^\circ \to e^+e^-$, the experiment also looks at the CP forbidden decay mode $K_L^\circ \to \pi^\circ e^+e^-$ and measures the polarization of μ^+ in the decay $K_L^\circ \to \mu^+\mu^-$. The physics interest in these processes has been discussed already in the chapter on CP violation. In addition, one should be also sensitive to $K_L^\circ \to \pi^\circ e\mu$, $e^+e^-\gamma$, $\mu^+\mu^-\gamma$, $4e$, $2\mu 2e$, etc.

I would like to end this chapter by emphasizing that if these proposed experiments can reach the advertised sensitivities, then they will be sensitive to propagators on the multi-TeV mass scale. In general, if these decays are mediated by some heavy object of mass m_H , then the rate for that decay is proportional to $f^2 f'^2 m_H^{-4}$ where the f's represent the coupling of the intermediate object at the 2 fermion vertices (see Fig. 28). Thus we have the simple relationship

$$\frac{\Gamma(K_L^\circ \to \mu e)}{\Gamma(K^+ \to \mu^+\nu)} \approx \left(\frac{ff'/m_H^2}{\sin\theta_c g^2/m_W^2}\right)^2$$

where g is the weak coupling constant and θ_c is the Cabibbo angle. Putting in known quantities we obtain:

$$m_H \approx 20\text{TeV}\left(\frac{10^{-8}}{BR(K_L^\circ \to \mu e)}\right)^{1/4}\left(\frac{ff'}{g^2}\right)^{1/2} .$$

Thus if $ff' \approx g^2$ and a $BR(K_L^\circ \to \mu e)$ of 10^{-12} can be reached, objects up to the masses of 200 TeV can be probed by those experiments.

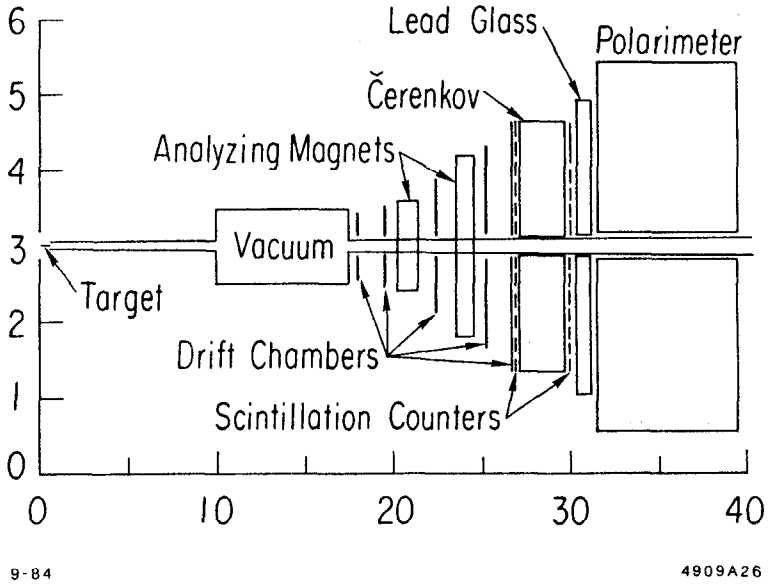

Figure 27 Schematic view of the E791 experiment. The dimensions are given in meters.

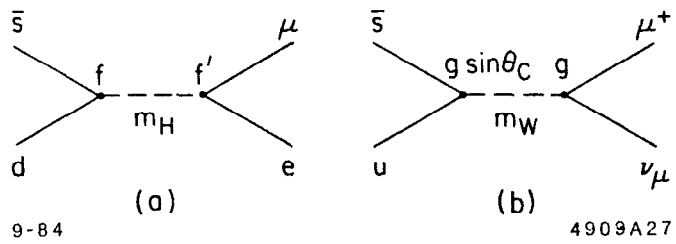

Figure 28 Comparison of the decays (a) $K_L^o \rightarrow \mu e$ mediated by a new heavy particle H and (b) $K^+ \rightarrow \mu^+ \nu$ mediated by the W boson.

5. LEPTON SECTOR

I would like to start this chapter by summarizing the status of our knowledge of the decays of the two heavy leptons, the μ and the τ. We have already mentioned in the previous section that the separate lepton number conservation, as tested in the muon decay, holds true to a very high level, approaching 10^{-10} in the branching ratios. A similar statement appears to hold true for the τ decays, although the experimental precision has not yet reached a comparable level. Specific neutrinoless τ decays have been looked for[75] with negative results, yielding following typical limits, e.g.

$$\begin{aligned} \tau &\rightarrow 3e \quad BR \quad < 4 \times 10^{-4}\,, \\ \tau &\rightarrow e\rho \quad BR \quad < 3.4 \times 10^{-4}\,, \text{ and} \\ \tau &\rightarrow \mu\gamma \quad BR \quad < 5.5 \times 10^{-4}. \end{aligned}$$

Other neutrinoless modes yield comparable upper limits.

Historically, muon decay has served as an ideal laboratory to study the weak interaction in some detail. Recent status has been summarized in a comprehensive review article by Scheck[76] and there have not been much new experimental input since that time. The Berkeley experiment[77] on the V-A nature of the μ decay will be discussed in the subsequent chapter on the searches for right-handed currents. One can summarize the μ decay situation with the statement that all of the data are consistent with the V-A interaction at a relatively high level of precision.

The τ decay provides another, considerably richer, area for the tests of our standard ideas of weak interactions. Within the standard model, the μ and τ decays should proceed by very similar diagrams illustrated in Fig. 29. The important difference stems from the fact that the τ is considerably heavier than the μ. This opens up the possibility of a number of different decay modes of the virtual W originating from the τ vertex. Thus a study of different τ decay modes is essentially a study of vertex B in Fig. 29 and represents a test as to whether

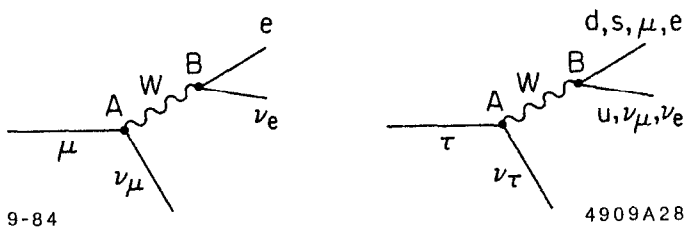

Figure 29 The μ and τ decay diagrams.

it is the standard W that is the sole mediator of the τ decay process. The net conclusion from all the data at hand is that no deviations from the standard picture have been observed here.

One can also look in detail at vertex A. A relatively old result[78] has shown that the τ decay is consistent with the V-A interaction. More specifically the Michel ρ parameter, predicted to be 0.75 for pure left-handed interaction has been measured to be 0.72 ± 0.10. The more recent experimental results have emphasized the measurement of the τ lifetime and hence the absolute strength of the $\tau - \nu - W$ vertex. The most recent comparison of the experimental value with the theoretical prediction yields[79]

$$\tau_\tau = (3.20 \pm 0.41 \pm 0.35) \times 10^{-13} \text{ sec} \qquad \text{experiment and}$$
$$\tau_\tau = (2.8 \pm 0.2) \times 10^{-13} \text{ sec} \qquad \text{theoretical prediction .}$$

Clearly, the experiment is in excellent agreement with the theoretical prediction. A better measurement of the τ leptonic branching ratios is needed if the comparison is to be pushed much further, since that is the limiting factor for the theoretical prediction.

We arrive thus at tentative conclusions based on the above experimental results that:

a) μ and τ are just "garden-variety" sequential leptons,

b) the separate lepton number is conserved to a high degree of accuracy.

Next we would like to consider to what extent other data might provide some additional information on the second statement. To elaborate on that we have to discuss briefly the formalism relevant to the lepton sector.

Given the fact that we have three lepton doublets, in analogy with the quark situation, namely,

$$\begin{pmatrix} e^- \\ \nu_e \end{pmatrix}, \begin{pmatrix} \mu^- \\ \nu_\mu \end{pmatrix}, \text{ and} \begin{pmatrix} \tau^- \\ \nu_\tau \end{pmatrix}.$$

We can ask whether the mass eigenstates in this sector are identical to the weak interaction eigenstates. As we discussed earlier, the answer to that question in the quark sector is an unequivocal NO. More formally, if we define

$|\nu_\alpha > \equiv$ neutrino "flavor" eigenstate (weak eigenstate) ,

$|\nu_i > \equiv$ neutrino mass eigenstate , and

$V \equiv$ lepton analogue of the K − M matrix

then we can write

$$|\nu_\alpha >= \sum_i V_{\alpha i} |\nu_i > \tag{5.1}$$

and the above question reduces to whether V is diagonal or not. Next, we shall explore the consequences that follow if V is <u>not</u> diagonal.

For simplicity we shall limit this discussion to the case of 2 flavors only. The 3 flavor situation has been discussed by several authors[80] in the literature. We have a mixing equation

$$\begin{pmatrix} \nu_e \\ \nu_\mu \end{pmatrix} = \begin{pmatrix} \cos\theta & \sin\theta \\ -\sin\theta & \cos\theta \end{pmatrix} \begin{pmatrix} \nu_1 \\ \nu_2 \end{pmatrix} \tag{5.2}$$

which relates the mass eigenstates to the flavor eigenstates by means of a lepton analogue of the K-M matrix. We consider a case when at $t = 0$ a pure flavor state is created, e.g. $|\nu_e >$. We can decompose it into mass eigenstates

$$|\nu_e >= \cos\theta \, |\nu_1 > + \sin\theta \, |\nu_2 > \qquad . \tag{5.3}$$

The mass eigenstates will have a time evolution that depends on their energy. Thus at some later time t we have a state

$$|\nu >_t = \cos\theta |\nu_1 > e^{-iE_1 t} + \sin\theta |\nu_2 > e^{-iE_2 t} \tag{5.4}$$

which can be transformed <u>back</u> to the $|\nu_e >, |\nu_\mu >$ basis to obtain:

$$|\nu >_t = (\cos^2\theta e^{-iE_1 t} + \sin^2\theta e^{-iE_2 t}) |\nu_e > + \cos\theta \sin\theta (e^{-iE_2 t} - e^{-iE_1 t}) |\nu_\mu > \ . \tag{5.5}$$

Thus we see that in general if a $|\nu_e >$ state is created at a time t=0 , at some

later time we shall have a finite probability of observing a $|\nu_\mu>$ state. We might thus be interested in two experimentally observable quantities:

a) probability of observing a $|\nu_e>$ state later on. This is defined as $P(\nu_e \rightarrow \nu_e) \equiv <\nu_e|\nu_e>_t$. Experiments looking for this phenomenon are called the "disappearance" experiments since in general the probability of observing ν_e will be less than 1.

b) probability of observing a $|\nu_\mu>$ state. Defined as $P(\nu_e \rightarrow \nu_\mu) \equiv <\nu_\mu|\nu_e>_t$, for only 2 neutrino states, this probability is given by $1 - P(\nu_e \rightarrow \nu_e)$. Experiments searching for ν_μ's in a beam originally composed of pure ν_e's are called "appearance" experiments.

Examining Equation 5.5 we see that the 2 necessary conditions for $P(\nu_e \rightarrow \nu_\mu) \neq 0$ are that $\theta \neq 0$ (i.e. matrix is non-diagonal) and that $E_1 \neq E_2$, implying that $m_1 \neq m_2$. It is convenient to express the latter requirement more explicitly. Taking advantage of the fact that $E >> m$, we can write

$$E_i \cong p + \frac{1}{2}\frac{m_i^2}{p} \approx E + \frac{1}{2}\frac{m_i^2}{E} \tag{5.6}$$

where E is the mean energy of the neutrino beam. Defining

$$\Delta = (E_i - E_j)t = \frac{\delta m^2}{2}\frac{L}{E}$$

with $\delta m^2 = m_i^2 - m_j^2$. With these approximations, we obtain

$$P(\nu_e \rightarrow \nu_e) = 1 - \sin^2 2\theta \frac{\sin^2 \Delta}{2} \text{ and} \tag{5.7a}$$

$$P(\nu_e \rightarrow \nu_\mu) = \sin^2 2\theta \sin^2 \frac{\Delta}{2} \ . \tag{5.7b}$$

Thus experiments on neutrino oscillations, if they yield negative results, can be interpreted as excluding a certain part of the $\sin^2 2\theta, \delta m^2$ space. We shall discuss them in more detail later, but first would like to review the independent evidence on the status of the masses of the three known (or expected) neutrinos.

Mass of the ν_e.

The classical reaction to investigate this question is the decay of tritium nucleus

$$H^3 \rightarrow He^3 + e^- + \bar{\nu}_e$$

with the electron kinetic energy endpoint (if $m_{\nu_e} = 0$) of 18.556 KeV. The technique relies on measuring the shape of the electron energy spectrum near the endpoint. The experiments of this kind present a number of challenges to the experimenters and are discussed in some detail in papers by Berquist.[81] Some of these problems are illustrated in Fig. 30. Since the nucleus changes its atomic number in the decay process, the final state He^3 ion can have its atomic electron not only in the ground state (n = 1), but also in (about 30% of time) one of the excited states (n = 2, 3, etc.) The difference in binding energy of these states reflects itself in the difference of masses of the whole system, and hence by energy conservation in the difference of endpoints of the decay electron energy spectrum. For example, the difference in binding energy between the lowest 2 states

$$M(^3He^+, n = 2) - M(^3He^+, n = 1) \approx 41eV$$

is of the same order as the typical energy resolution of the experiments. In reality, the actual situation is even more complicated, since the source used in neutrino mass experiments is not atomic tritium but part of some complicated molecule. Thus molecular physics must be well understood to interpret the results.

As seen in Fig. 30 a non-zero neutrino mass will result in curvature of the spectrum that is concave downward. But experimental resolution effects will smear this distribution and give it a curvature that is concave upward. Thus an overestimate of experimental errors can result in a false assignment of non-zero neutrino mass.

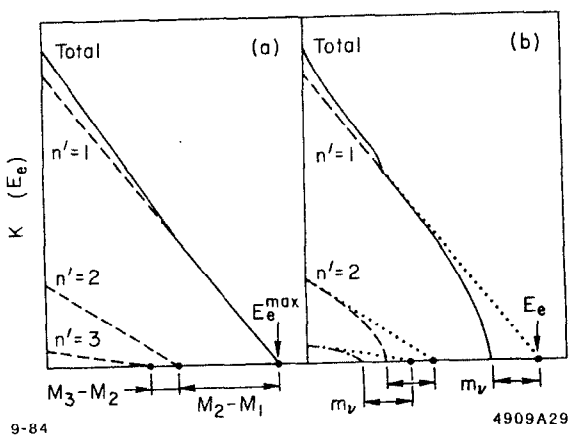

Figure 30 Detailed endpoint shape of the Kurie plot for atomic tritium β decay: (a) case of $m_\nu = 0$, and (b) case of $m_\nu \neq 0$. Effects of experimental resolution are not included (from Ref. 85).

The interest in the m_{ν_e} question has been revived recently by the experimental results from the ITEP group who in 1980 found[82]

$$14 < m_{\nu_e} < 46 \text{ ev} \qquad (99\% \text{ C.L.}) ,$$

i.e. evidence for a non-zero electron neutrino mass. The group has recently repeated their experiment with improved resolution, lower background, and higher counting rate.[83] The optimum m_ν value for the assumption of molecular valine (source of tritium in the ITEP experiment) final states is 33 ± 1 ev, but the hypotheses of molecular and atomic tritium states also give non-zero electron mass values. The edge of the experimental spectrum is shown in Fig. 31 with $m_\nu = 33$ ev and $m_\nu = 0$ hypotheses superimposed. The χ^2 for $m_\nu = 33$ ev is rather poor, 522 for 295 degrees of freedom, indicating that some systematic sources of error still need to be understood.

Recently J. J. Simpson raised the objection[84] that the calibration line used by the ITEP group to calculate their resolution has its own Lorentzian width of 9 ev; this fact was apparently overlooked by the experimenters. He claims that including this correction properly would decrease the resolution sufficiently to allow the zero mass hypothesis within the 90% C.L.

The ITEP results stimulated sufficient interest so that a large number of other groups around the world are attempting this experiment. The salient facts of the proposed experiments are reproduced below in Table IV, extracted from Shaevitz's review talk.[83]

A new approach to the problem of ν_e mass has been recently proposed by A. DeRujula[85] who suggested using a radiative electron capture process. In this process the final state consists of a nucleus, neutrino and the photon, and the measurement of the photon energy near its endpoint can give a value of the neutrino mass. The detection of photons in this energy range can be somewhat cleaner than detection of electrons, because there is no energy loss in the target in the photon case. On the other hand the counting rate at the endpoint is

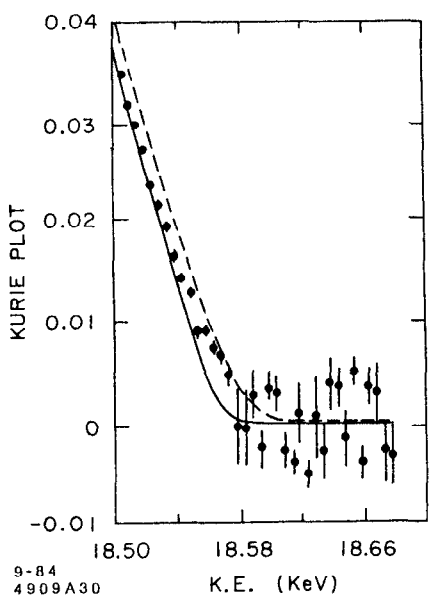

Figure 31 The edge of the Kurie plot from the 1983 ITEP experiment. The solid line is the best fit to the $m_\nu = 33$ ev hypothesis; the dashed line assumes $m_\nu = 0$.

strongly suppressed. DeRujula suggested overcoming this difficulty by using a substance that has an atomic resonance in the vicinity of the endpoint which could significantly enhance the rate in this region. The proposed best candidate isotope was ^{168}Ho and an experimental program has been initiated[86] to study this decay.

Table IV

Future β-Decay Experiments

Experiment	Source	Resolution (rms)	Sensitivity (m_{ν_e})
Fackler et al. Rock-FNAL-LLL	Solid Molecular ^3H	1-2 eV	> 4 eV
Boyd, Ohio State	Solid Molecular ^3H	10 eV	> 10 eV
Bowles et al., LAMPF	Atomic ^3H	40 eV	> 10 eV
Clark, IBM	Solid ^3H	5 eV	–
Heller et al. UC Berkeley	^3H in Semi-conductor	100 eV	> 30 eV
Graham et al. Chalk River	–	10 eV	>~ 20 eV
Bergkvist	^3H in valine	~ 25 eV	> 19 eV
Kundig, Zurich	–	5 eV	> 10 eV
INS, Japan	–	13 eV	> 25 eV

Finally one should mention that recently a K capture with a very low Q value, 156 ± 17 ev, has been discovered in ^{158}Tb isotope.[87] Raghaven has estimated that one could measure neutrino mass in this process down to 25 ev in the first generation mass experiments.

Mass of the ν_μ.

The measurement of ν_μ mass is intrinsically more difficult because no channels exist where the energy released is low. Traditionally, the two optimum processes to study this problem have been the decays

$$K_L^\circ \rightarrow \pi^\pm \mu^\mp \nu_\mu \qquad (5.8)$$

and $$\pi^+ \rightarrow \mu^+ \nu_\mu \, . \qquad (5.9)$$

The history of upper limits on ν_μ mass has been summarized by Shaevitz and is illustrated in Fig. 32. Channels 5.8 and 5.9 have alternated as sources of the best upper limit at any given time. The π decay has the advantage that the Q of the decay is about an order of magnitude lower. However, being a two body decay, the mass of the neutrino enters as the square into the energy balance equation. The K° decay channel suffers from a high Q value and the fact that the useful events, i.e. those with neutrino taking a negligible fraction of the total energy, are strongly suppressed by phase space factor.

The present best upper limit is

$$m_{\nu_\mu} \leq 0.49 \text{ MeV} \qquad (90\% \text{ C.L.})$$

and comes[88] from the study of the momentum of the decay muon from a π^+ at rest.

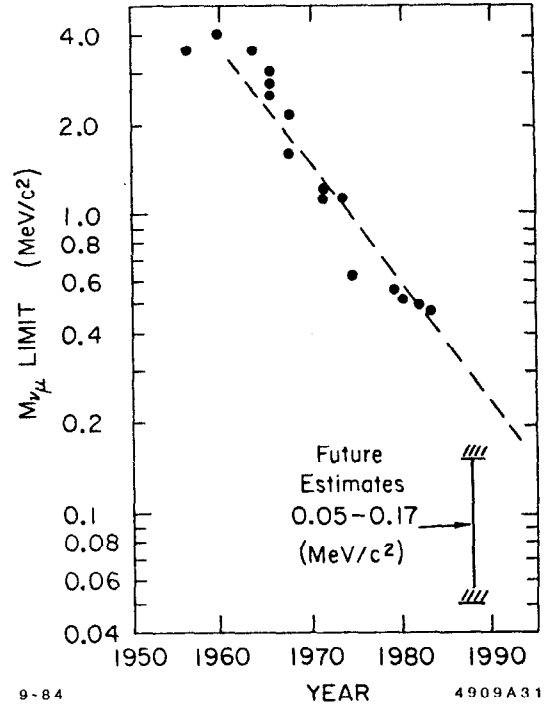

Figure 32 Muon neutrino mass limits as a function of time.

Mass of the ν_τ.

Similar difficulties, but considerably magnified, are also present in the ν_τ mass experiments. Here most useful are the τ decay channels where the observable final state products have as high a mass as possible. The present record holder is the reaction

$$\tau^{\pm} \rightarrow \pi^+\pi^{\pm}\pi^-\pi^0\nu_\tau \qquad (5.10)$$

since the 4π mass state can have high effective mass due to the ρ' intermediate state. The data on this question from the MarkII collaboration[89] is shown in Fig. 33. The quoted upper limit on the ν_τ mass is

$$m_{\nu_\tau} < 164 \text{ MeV} \qquad (95\% \text{ of C.L.}) \, .$$

Further progress on the ν_τ mass will have to await new techniques and new channels. Thus, for example, the decay modes

$$D(\text{or } F) \rightarrow \tau + \nu_\tau \qquad (5.11)$$

would be useful, if sufficient number of events could be obtained, because of the relatively low Q value. Similarly the rate for the decay

$$K^+ \rightarrow \pi^+\nu_\tau\bar{\nu}_\tau \qquad (5.12)$$

is obviously very sensitive to the ν_τ mass since the total energy released, and available for the two ν's is only 354 MeV.

Subdominantly coupled ν's.

We have already mentioned that non-zero ν masses and a non-diagonal V matrix can be detected through ν oscillations. Shrock[90] has pointed out that these phenomena can also be searched for by looking for multiple peaks in the

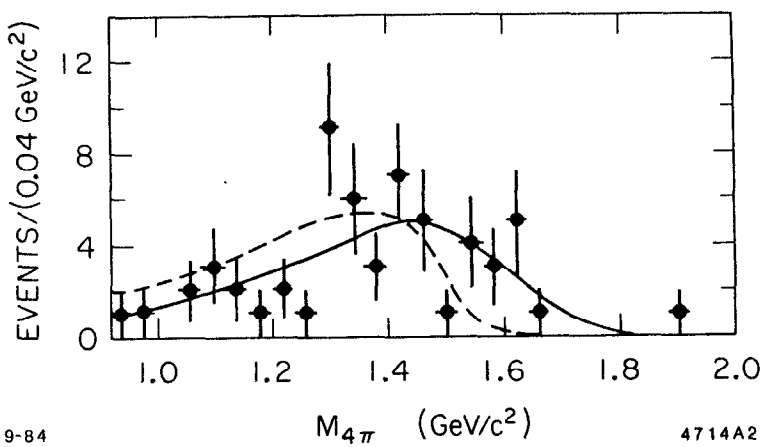

Figure 33 The 4π invariant mass distribution from the $\tau \rightarrow 4\pi + \nu$ decays. The solid line assumes $m_{\nu_\tau} = 0$, the dashed line $m_{\nu_\tau} = 250$ MeV. Both curves are drawn with the assumption of ρ' dominance with a mass of 1570 MeV and a width of 510 MeV.

lepton momentum spectrum in π and K decays. Thus if neutrino flavor states are written

$$\nu_\alpha = \sum_i V_{\alpha i} \nu_i \tag{5.13}$$

and if all the ν_i have different masses and if they are all kinematically accessible to a given decay, then this decay will exhibit as many peaks in the lepton momentum spectrum as there are neutrino mass states.

An analogous situation exists in the τ decay, where the 2 body decay can be written as

$$\tau^- \to \nu_\tau + (\bar{u}d') \tag{5.14}$$

and d', the weak interaction eigenstates is given by

$$d' = U_{ud}d + U_{us}s + U_{ub}b\ . \tag{5.15}$$

Because the decay into the b quark is energetically forbidden, we shall see <u>two</u> monoenergetic ν_τ peaks in τ decay corresponding to

$$\begin{aligned} &\tau^- \to \nu_\tau + (\bar{u}d) \ \text{ i.e. } \ \tau^- \to \pi^- + \nu_\tau \\ \text{and} \quad &\tau^- \to \nu_\tau + (\bar{u}s) \ \text{ i.e. } \ \tau \to K^- + \nu_\tau\ . \end{aligned} \tag{5.16}$$

An alternate technique to look for the same phenomena is to search for decays of heavy neutrinos in a neutrino beam. Thus if a K decay would result in a mixture of ν_μ's and some other heavy neutrino ν_H, we might expect to see subsequently

$$\nu_H \to \nu_\mu e^+ e^-\ .$$

Comprehensive discussions of these searches have been given by Shaevitz[83] and Winter[91] and will not be repeated here. No positive results have been found and the experiments can be interpreted as correlated upper limits on the mass of the heavy neutrino and the strength of mixing $|V_{\alpha i}|^2$. The limits on couplings to the electron and muon neutrino are reproduced in Fig. 34.

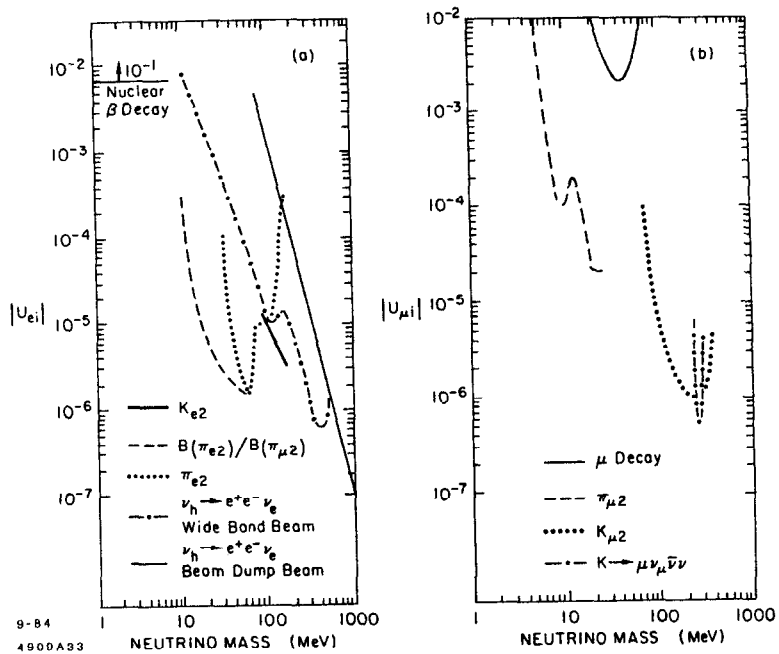

Figure 34 Limits on masses and couplings of heavy neutrinos to electron neutrinos (a) and muon neutrinos (b).

ν oscillations - general comments.

Before we discuss the ν oscillations experiments in detail, some general comments might be in order. First, we should again emphasize that all of the analyses to be discussed assume a two neutrino picture. Second, as we discussed previously, the figure of merit for the sensitivity of any experiment to the potential oscillations is the parameter Δ defined as

$$\Delta = \frac{\delta m^2}{2}\frac{L}{E} \quad . \tag{5.17}$$

It is convenient to identify three general ranges of Δ, i.e.

a) $\Delta << \pi$, corresponding to a situation where we are still close enough to the neutrino source so that the oscillations have not yet had sufficient time to develop. These experiments will be very insensitive to ν oscillations.

b) $\Delta \approx \pi$, corresponding to the optimum experimental situation for ν oscillation searches. Within the energy band of ν's accepted by the experiment, one can expect significant differences in behavior due to oscillations.

c) $\Delta >> \pi$, corresponding to the situation where the ν beam went already through several oscillation wavelengths. This will result in an inability to see the differences in behavior of ν's of different energies because in general we shall be integrating over too large a bandwidth. These experiments will still be sensitive to "disappearance" phenomena provided that $\sin^2\theta$ is large enough and our a priori knowledge of the flux good enough.

The neutrino oscillation experiments can be conveniently grouped into several categories, depending on the ν sources:

a) solar neutrino experiments. These have the advantage of large L/E but poor knowledge of the initial intensity. Thus they are sensitive to very small δm^2 , but only to large values of $\sin^2\theta$.

b) cosmic ray neutrino experiments. Similar comments apply here as to solar ν's, but L/E is typically lower; primary flux information could in principle be better. The neutrinos studied here are ν_μ's as opposed to solar neutrinos that are ν_e's.

c) reactor experiments. These give rise to $\bar{\nu}_e$'s with reasonably large L/E and high intensities. There is some flux uncertainty associated with many fission products that subsequently undergo β decay.

d) accelerator experiments. Those are characterized by the optimum control of the source, but rather small possible L/E values.

The various experiments (present and future) on ν oscillations have been summarized by Silverman and Soni.[92] The range that they cover in the L-E_ν space, together with their δm^2 sensitivity is shown in Fig. 35.

Solar neutrinos.

The detection of solar neutrinos on earth presents one possible method of searching for neutrino oscillations. The experiment relies on the fact that the sun is an intense source of electron neutrinos. These ν_e's have an energy low enough so that if they are transformed into ν_μ's or ν_τ's , the latter have too low an energy to participate in charged current reactions. Hence, ν oscillations will exhibit themselves as a deficiency of the detected neutrinos.

The experimental method relies on detecting the capture reaction

$$\nu_e + {}^{37}Cl \rightarrow {}^{37}Ar + e^- \tag{5.18}$$

in a large tank of liquid C_2Cl_4. The ^{37}Ar atoms are removed from the vessel by purging with helium gas and subsequently detected via their K capture reaction. The experimental details are described extensively in the available literature.[93]

The main advantage of this experiment is a very large L/E value giving rise to potential sensitivity down to a very small $\delta m^2 (\sim 10^{-11}\text{ev}^2)$. On the other hand, as mentioned previously, the sensitivity to $\sin^2 2\theta$ values is rather poor, due to theoretical uncertainties associated with the intensity of the source. The reason for the latter is illustrated in Table V which gives the reactions responsible for

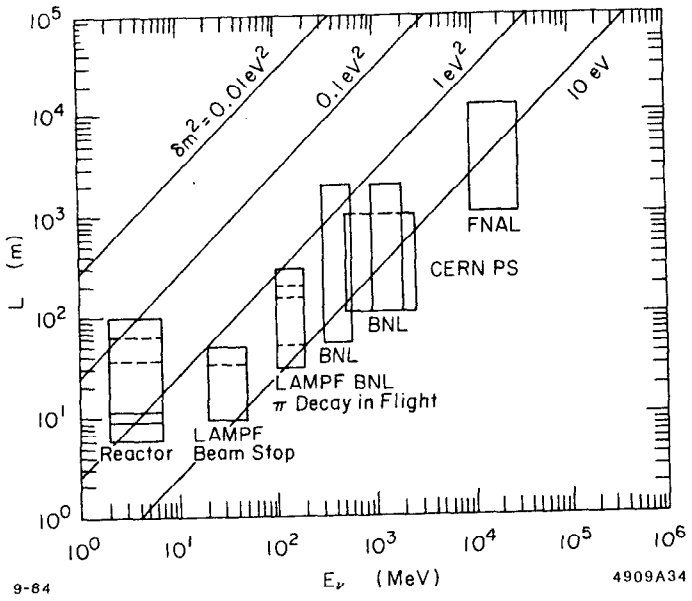

Figure 35 The neutrino source to detector distance (L) vs neutrino energy (E_ν) for various neutrino oscillation experiments together with their approximate sensitivity to the mass difference squared δm^2.

Table V

Neutrino Sources

Reaction	Energy (MeV)	Predicted Flux $10^{10}cm^{-2}sec^{-1}$	SNU (^{37}Cl)
$p + p \rightarrow D + e^+ + \nu_e$	0 - 0.4	6.1	0
$p + e^- + p \rightarrow D + \nu_e$	1.4	0.015	0.23
$^7Be + e^- \rightarrow {}^7Li + \nu_e$	0.86(90%) 0.34(10%)	0.34	1.03
$^8B \rightarrow {}^8Be^* + e^+ + \nu_e$	0 -14	0.00060	6.48
$^{13}N \rightarrow {}^{13}C + e^+ + \nu_e$	0 - 1.2	0.045	0.07
$^{15}O \rightarrow {}^{15}N + e^+ + \nu_e$	0 - 1.7	0.035	0.23
			8.04

the solar neutrinos, their energy and the expected contribution to the counting rate in a ^{37}Cl detector.[94] The unit that is convenient to use here is an SNU, a standard neutrino unit, defined as

$$1 \text{ SNU} \equiv 10^{-36}\nu_e \text{ captures/sec/target nucleus}(^{37}Cl) .$$

The difficulty lies in the fact that the threshold for the ^{37}Ar production is 0.814 MeV, and thus the majority of the ν_e flux from the sun is not able to contribute to the reaction in question. Hence the theoretical interpretation of the experimental results depends very strongly on our understanding of the production mechanisms of the high energy tail of the neutrino spectrum.

The experimental program of R. Davis et al.[95] has been going on now for over a decade. Their annual results until 1978 and the latest average are shown in Fig. 36. The average value of 2.2 ± 0.4 SNU is considerably lower than the theoretical prediction of 8.0 ± 3.3 SNU[94] obtained by summing over all the reactions listed in Table V. Whether this discrepancy is due to theoretical uncertainties in the solar neutrino flux calculations or new physics is unclear at the present time.

There has been a significant interest lately in exploring other avenues to probe this question, specifically by utilizing nuclear neutrino induced reactions with a significantly lower threshold.[94] One specific channel that has attracted a lot of attention is the $^{71}Ga\ (\nu, e)\ ^{71}Ge$ reaction that has a threshold of 0.236 MeV. Its relative advantage over ^{37}Cl reaction is well demonstrated when one compares the detection threshold energy with the energy spectra resulting from all of the solar reactions generating electron neutrinos (see Fig. 37). The total calculated rate for a ^{71}Ga target is 102 SNU's, considerably higher than for the ^{37}Cl reaction.

Cosmic ray neutrinos.

The cosmic ray hadronic showers are a source of muon neutrinos by virtue of the decay process $\pi \rightarrow \mu\nu$, where the pions come from the hadronic cascade initiated by the primary cosmic rays. Furthermore, the muon rate and spectrum observed on the earth's surface allow us to calculate the ν_μ flux and the energy distribution, since both μ's and ν_μ's come from the same source. The ν_μ flux can be measured in principle by observing ν_μ interactions in detectors located deep underground so that they will be shielded from other nuclear interactions. In practice, the fluxes are so low that one is forced to use the earth above the detector as the target, the detector serving only to observe the μ's resulting from the ν_μ interactions. Any deficiency of the μ's would constitute evidence of possible ν oscillations since ν_e interactions would give no μ's and ν_τ's only a much reduced number of μ's (from τ decay).

The experimental difficulty lies in the fact that the μ detectors discussed

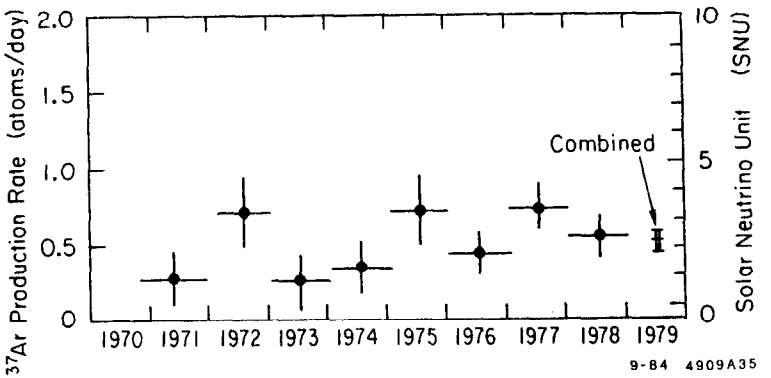

Figure 36 The annual average ^{37}Ar production rate from the experiment of R. Davis et al. The combined average is indicated on the right.

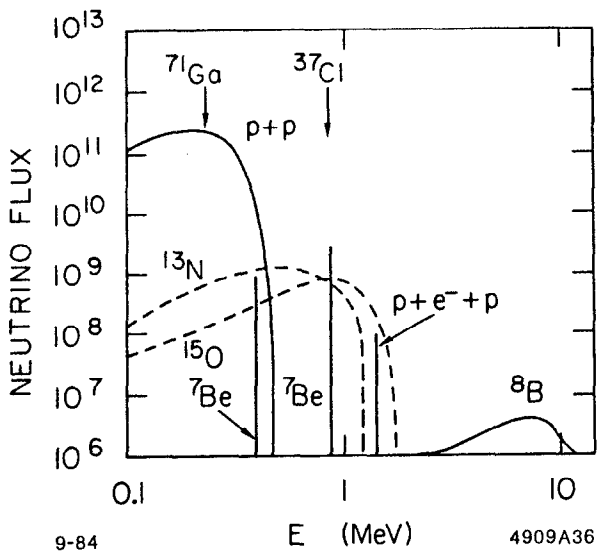

Figure 37 Energy spectrum of the solar neutrinos as indicated by the standard model. The thresholds for ^{37}Cl and ^{71}Ga reactions are indicated by the arrows. The fluxes are given in cm^{-2} sec^{-1} MeV^{-1} for continuum sources and in cm^{-2} sec^{-1} for line sources.

above will also be sensitive to the most energetic μ's that originate in the atmosphere from π decay and have enough energy to penetrate to the detector. That component can be separated out if one looks at the zenith angle distribution of the observed μ's. At large zenith angles the primary μ's will have to go through a large amount of earth; thus at those angles only μ's produced by ν_μ interactions should be present. Alternatively, if the detector can identify the direction of the muon by time of flight technique, it can isolate upward going μ's, i.e. those coming from interactions of ν_μ's originating from π decays on the other side of the earth. Those μ's should have no contamination from primary muons. All three of these sources are indicated very schematically in Fig. 38.

The results of the experimental observations and theoretical predictions are compatible with each other within experimental errors. Two of the underground setups[96] that do not measure time of flight give fluxes of neutrino induced muons that are mutually compatible and yield

$$I_\mu^{\text{theor}}/I_\mu^{\text{exp}} = 1.6 \pm 0.4 \ .$$

The Baksan-Valley experiment in the Soviet Union that does measure the time of flight obtains[97]

$$I_\mu^{\text{theor}}/I_\mu^{\text{exp}} = 1.0 \pm 0.26 \ .$$

Finally, a Soviet underwater muon detector,[97] operating at depths of 2000 m, 3000 m, and 3700 m finds

$$I_\mu^{\text{theor}}/I_\mu^{\text{exp}} = 1.19$$

based on 350 observed events.

The new generation proton decay detectors can in principle investigate this question in considerably more detail. The early results from the IMB experiment[98] are consistent with theoretical calculations: 69 events have been found, all of which are consistant with being due to ν interactions; 95 ± 30 are predicted.[99]

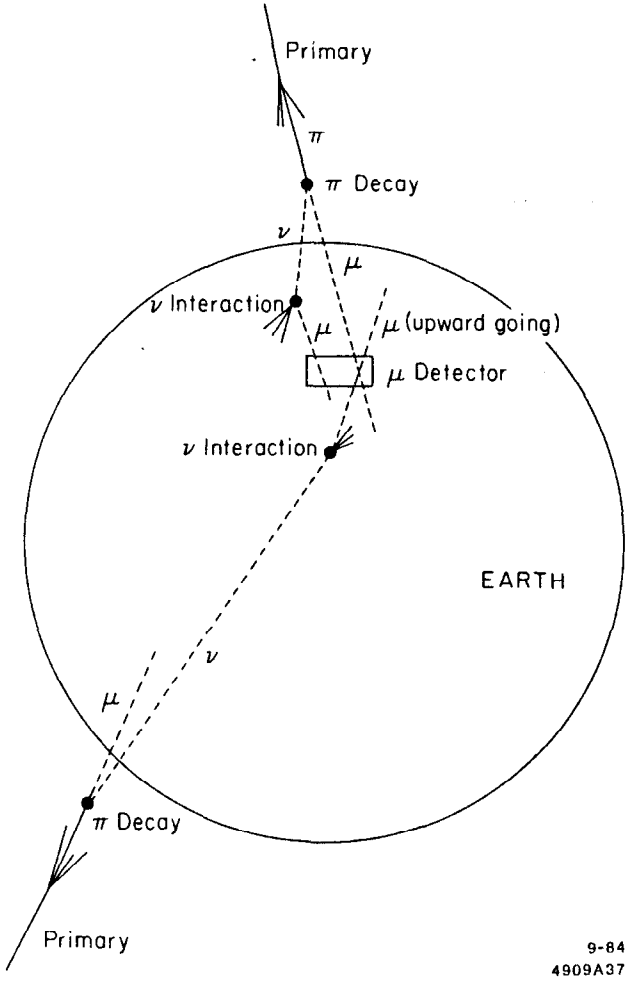

Figure 38 Schematic drawing of potential sources of μ's detected by an underground muon detector.

It should be pointed out, however, that this experiment is sensitive also to ν_e interactions as opposed to the μ detector experiments that can see only ν_μ's. Thus the results of these two kinds of experiments are not directly comparable.

Accelerator experiments.

The experimental input on the question of ν oscillations from the accelerator experiments can most naturally be classified into several different sources:

a) beam dump experiments,

b) disappearance experiments and

c) appearance experiments.

The beam dump experiments detect mainly "prompt" neutrinos, i.e. neutrinos originating from sources that have mean decay paths small compared to the typical interaction lengths. Various techniques are used to suppress and/or calculate the background from ν's resulting from π and K decays.

The dominant source of prompt neutrinos are expected to be charmed particle decays, predominantly decays of D° and $D^\pm$. Because of $\mu - e$ universality, the number of ν_μ and ν_e interactions should be the same, except for small phase space correction in the D decay process. Thus deviation from unity in the observed ν_e/ν_μ interaction ratio might be evidence for oscillation phenomena. The latest results have been recently reviewed by K. Winter[91] and are summarized in Table VI. Except for the anomaly observed by the CHARM experiment, the experiments are consistent with equal rates of ν_μ and ν_e interactions.

Table VI

Summary of the 1982 results on the ratio of electron- and muon-neutrino fluxes

Experiment	Electron ident. method*)	E_ν cut	$\phi(\bar{\nu}_e + \nu_e)/\phi(\bar{\nu}_\mu + \nu_\mu)$ (a)
CHARM	direct (extrap.)	2 GeV	$0.57 \pm {}^{0.11}_{0.10} \pm 0.07$
CHARM	subtraction (extrap.)	2 GeV	$0.59 \pm {}^{0.11}_{0.10} \pm 0.08$
CDHS	subtraction (extrap.)	20 GeV	$0.83 \pm 0.13 \pm 0.12$
BEBC	direct (subtraction and extrapol.)	20 GeV	$1.35 \pm {}^{0.65}_{0.34} \pm 12\%$
FMOW	direct	20 GeV	$1.09 \pm 0.10 \pm 0.10$
FMOW	subtraction (subtraction and extrap.)	20 GeV	$1.02 \pm 0.09 \pm 0.10$

(a) First error is statistical, second error is systematic.

*) In parenthesis is indicated the method used for determining the prompt fluxes.

There has been recently a renewed interest in dedicated accelerator experiments to search for ν disappearance phenomena.[100] These generally use two different (but as similar as possible) detectors located at two different distances from the neutrino source. Both of the detectors take data at the same time and are illuminated by the same neutrino beam. Thus sensitivity to detection efficiency and Monte Carlo calculations is considerably lessened. These experiments are generally sensitive to relatively large values of δm^2 (tens of eV^2) and moderate values of $\sin^2 2\theta (\gtrsim 0.1)$. The neutrino oscillations in these experiments would show up as a variation in the ratio of rates in the forward to backward detector as a function of ν energy that could not be explained by the relatively minor effects having to do with slightly different detection efficiencies in the two detectors. The results so far have been negative, yielding no evidence for neutrino oscillations. A typical result (from the CDHS experiment, Ref. 100) is shown in Fig. 39. The summary of all the experimental data will be presented at the end of this chapter after discussion of the reactor data.

The appearance experiments that have been performed so far can be classified into either $\nu_\mu \to \nu_e$ or $\nu_\mu \to \nu_\tau$ variety. They require clean beams without any original contamination of the potentially regenerated neutrino species. So far only ν_μ beams have satisfied this condition since the pure $\bar{\nu}_e$ beams from the reactors are too low in energy to be able to produce μ's or τ's if $\nu_e \to \nu_\mu$ or $\nu_e \to \nu_\tau$ transitions exist. The detectors for these experiments must have good spatial resolution because of the need to identify e's and τ's. Thus emulsions, bubble chambers and fine grain electronic detectors have made the principal contributions in the area. No evidence for neutrino oscillations have been seen in any of these experiments.

Reactor experiments.

Because of the very high fluxes and low energy, these experiments can probe rather low region of δm^2. The early experiments[101] concentrated on comparison of the experimental results on neutrino interaction rates and spectra with theoretical predictions; more recently, there has been a trend to dedicated oscillation experiments that operate the neutrino detector at two or more positions and thus can perform a relative rate measurement.

The Cal Tech - ISN Grenoble (later SIN) - TU Munich collaboration initiated their studies[102] at the ILL Grenoble reactor working at a distance of 8.75 m from the reactor core. They identify the reaction

$$\bar{\nu}_e p \to e^+ n$$

by detecting both the positron and the neutron in a coincidence. Aside from a small neutron recoil energy correction the neutrino energy is given by

$$E_{\bar{\nu}} = E_{e^+} + 1.8 MeV$$

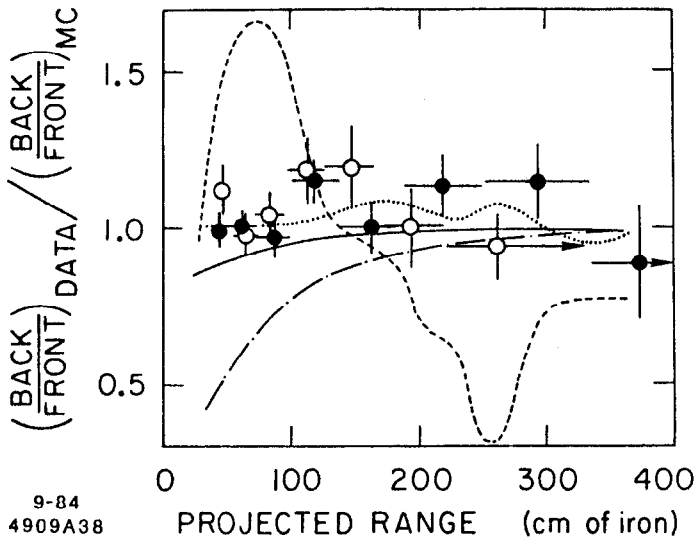

Figure 39 Ratio of Monte Carlo corrected event rates in the back and front CDHS detector as a function of projected range in iron. Also shown are curves indicating the expected behavior of these ratios in the case of oscillations for different choices of δm^2 and $\sin^2 2\theta$. Solid curve $\delta m^2 = 1$ eV^2 and $\sin^2 2\theta = 0.2$; dash-dotted curve $\delta m^2 = 1$ eV^2 and $\sin^2 2\theta = 1$; dotted curve $\delta m^2 = 32$ eV^2 and $\sin^2 2\theta = 0.2$; dashed curve $\delta m^2 = 16$ eV^2 and $\sin^2 2\theta = 1$. Solid circles refer to interactions in fine grained modules; open circles to the more coarse modules.

and thus a measurement of positron energy ($\delta E/E = 0.35\sqrt{E}$) yields the observed neutrino energy spectrum.

More recently this experiment has been continued[103] at the high power Gösgen reactor in Switzerland. Data were taken at 2 distances, 37.9 m and 45.9 m, allowing a test for the existence of neutrino oscillations independent of the knowledge of the neutrino flux. In addition, the data at the two positions can be combined and compared with the calculated ν_e spectrum that is based on the measured β decay spectrum from ^{235}U and ^{239}Pu. Neither one of the two analyses gives any evidence for the oscillations,[104] the combined data analysis yielding somewhat more restrictive limits on δm^2 and $\sin^2 2\theta$.

The LAPP, Annecy - ISN, Grenoble group recently presented results[105] from a high statistics experiment at the Bugey reactor in France. The neutrino flux at 13.6 m distance is $2 \times 10^{13}/\text{cm}^2/\text{sec}$, which is the highest intensity presently available for any experiment near a reactor. The experimental technique is very similar to that used by the other collaboration. The detector consists of liquid scintillator and ^3He proportional chamber sandwiches; the former is used to detect positrons and measure their energy, the latter to detect the neutron via the capture reaction

$$n + {}^3He \rightarrow t + p\,. \tag{5.19}$$

About 63000 $\bar{\nu}_e$ events have been observed at 2 different detector locations, 13.6 and 18.3 m away from the reactor core. The group have observed a difference in the counting rate and in the apparent energy spectrum at the two locations.

The measured ratio of fluxes at the two positions, as a function of positron energy is displayed in Fig. 40. The ratio appears not only to be different from unity, but also to have some energy dependance. The allowed region in the δm^2, $\sin^2 2\theta$ space, if this effect is interpreted as due to ν oscillations, is shown in Fig. 41. If we compare these results to the data from the Gösgen reactor, 2 location experiment, we find that values of the parameters $\delta m^2 \approx 0.2$ and $\sin^2 2\theta \approx 0.2$

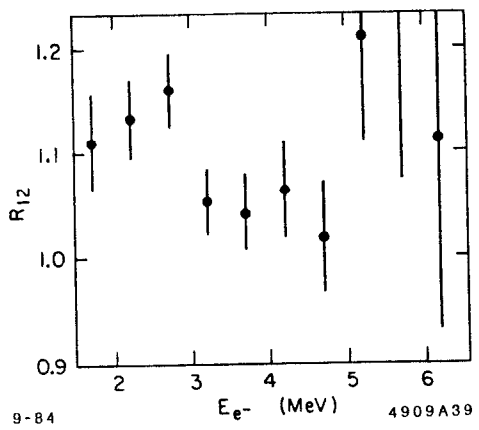

Figure 40 The ratio of $\bar{\nu}_e$ fluxes, as measured by $\bar{\nu}_e$ interactions, at the 2 locations in the Bugey experiment.

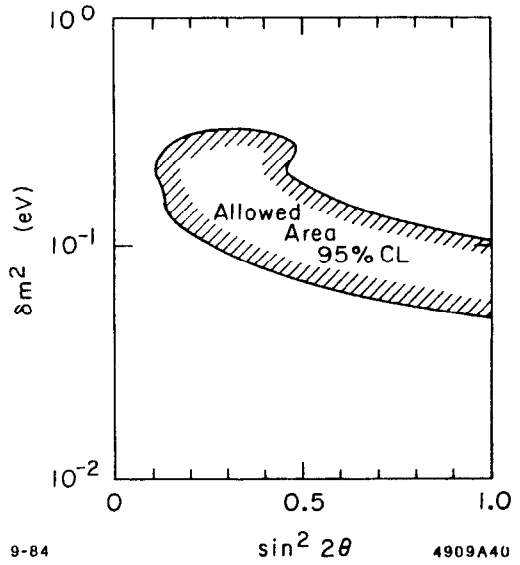

Figure 41 The parameter space allowed by the Bugey experiment, if the results are interpreted as due to ν oscillations.

are mutually compatible. On the other hand, the Bugey results contradict the Gösgen limits obtained by comparing the experimental results with the spectrum predicted from the experimental study of U and Pu fission and their byproducts.

ν oscillations - summary.

The best experimental upper limits for the correlated values of δm^2 and $\sin^2 2\theta$ are shown in Figs. 42 and 43. Figure 42 illustrates the upper limit envelopes extracted from all of the inclusive experiments (i.e. disappearance). Figure 43 shows the upper limit envelopes for the exclusive channels $\nu_\mu \to \nu_e$ and $\nu_\mu \to \nu_\tau$. If the inclusive limits are more stringent than the exclusive ones, the former are used in Fig. 43. One should emphasize once again, that these limits were obtained in the framework of the 2 neutrino flavor picture. The curves come mainly from Shaevitz's review talk[83] and have been updated by the most recent results.[100] The Bugey reactor experiment results are not included in these figures.

Double β decay.

The double β decay process

$$Z \to (Z-2) + 2e^- + 2\nu_e \tag{5.20}$$

occurs in nature by virtue of the fact that the expression for the mass of a nucleus has a term which depends on whether we are dealing with an odd-odd or even-even nucleus. Thus the mass of even A nuclei is described by two different curves, as exhibited in Fig. 44. The process (5.20) is not very interesting from the particle physics point of view since it merely represents a simultaneous beta decay of two d quarks. It does, however, present a rather formidable calculational problem to theoretical nuclear physicists.[106]

From the particle physics point of view, a very interesting question is whether the neutrinoless double β decays exist, namely the process:

$$Z \to (Z-2) + e^- + e^- \tag{5.21}$$

without the emission of any neutrinos. Very schematically, this decay would have

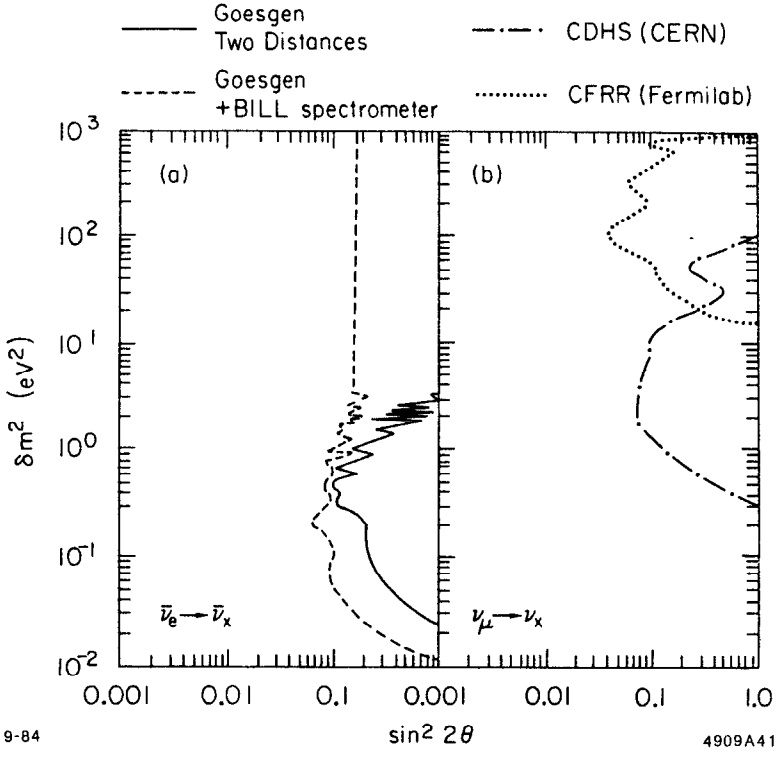

Figure 42 Upper limits on δm^2 and $\sin^2 2\theta$ obtained from the inclusive (disappearance) experiments.

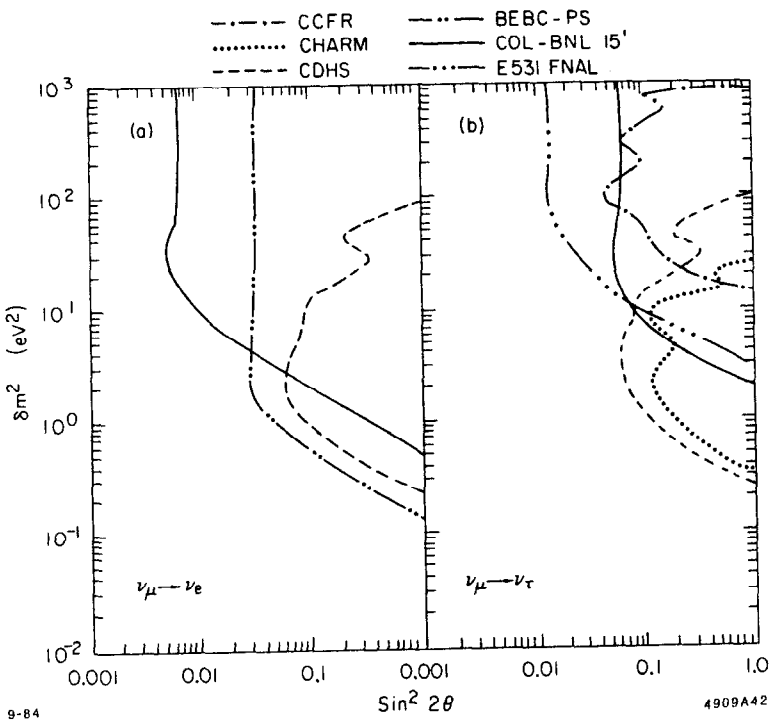

Figure 43 Upper limits on δm^2 and $\sin^2 2\theta$ obtained from the exclusive (appearance) experiments.

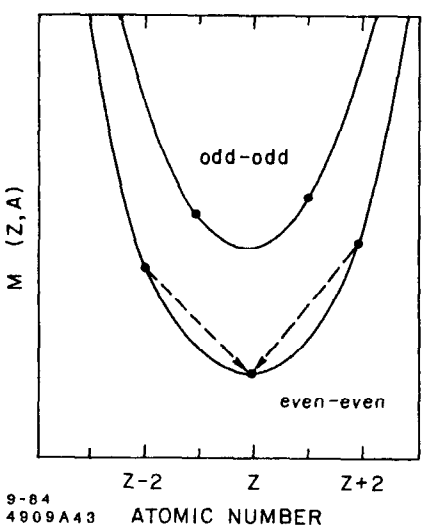

Figure 44 Energy systematics of even A nuclei. An allowed double β decay is indicated by an arrow.

to proceed as indicated in Fig. 45. In the conventional picture, since the same neutrino is both emitted and absorbed by the W^-, the process is forbidden both by lepton number conservation and helicity. Thus for the decay to proceed, the neutrino must be a Majorana particle, namely $\nu \equiv \bar{\nu}$ and the helicity requirement has to be somewhat relaxed. The latter can be accomplished in two ways: either by giving the neutrino some mass or by allowing some right-handed currents. The experimental implication of that fact is that negative results on neutrinoless double beta decay can be translated into correlated limits on neutrino mass and admixture of right-handed currents for a Majorana neutrino. The latter is usually parametrized by the ratio η of the masses squared of the two relevant vector bosons, namely

$$\eta \equiv |\frac{M_{W_L}}{M_{W_R}}|^2 . \tag{5.22}$$

Experimentally, there are several different experimental approaches to this question. The oldest technique relies on the geochemical means, namely detection by chemical analysis of the daughter nuclei trapped in the ores rich in the parent nuclei. Besides many serious difficulties connected with the proper interpretation of the source of the daughter nuclei, the method has two other very serious disadvantages. First, it cannot separate out the 2ν from 0ν decay modes but measures only the total rate, λ_T , i.e.

$$\lambda_T \equiv \lambda_{2\nu} + \lambda_{0\nu} . \tag{5.23}$$

This evidence for a non-zero $\lambda_{0\nu}$ comes from detection of excess of the daughter nuclei over and above what one would expect from the conventional 2ν double beta decay rate. This is where the second difficulty comes in, namely the necessity to rely on theoretical calculations to calculate $\lambda_{2\nu}$. As we mentioned previously, these calculations are difficult and those available in the literature show serious discrepancies.

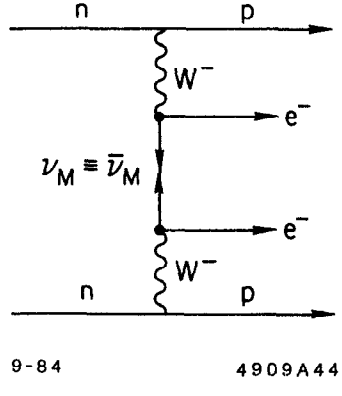

Figure 45 A diagram representing a neutrinoless double beta decay.

On the other hand the situation is somewhat helped by the phase space considerations. Since the energy released in a typical double beta decay is quite low, the phase space effects enhance the 2 body decay (no-ν decay) considerably - typically by a factor of $\sim 10^6$ relative to the conventional 4 body decay.

It has been pointed out by Pontecorvo[107] that these considerations lead one to conclude that considerable improvement in the accuracy of the final answer could be obtained if decay-rate ratios of pairs of similar nuclei are studied. The ratio of their respective nuclear matrix elements should be near unity, and generally, because of different phase space factor, the 0ν decay mode in one of the 2 channels would be significantly enhanced. Thus for example if one considers ^{128}Te and ^{130}Te, the Q values are 869 and 2533 keV respectively. Thus $\rho_{0\nu}$, defined as

$$\rho_{0\nu} \equiv {}^{128}\lambda_{0\nu} / {}^{130}\lambda_{0\nu}$$

will be much greater than $\rho_{2\nu}$, defined accordingly. Thus the overall ratio, $\rho_T >> \rho_{2\nu}$ if the neutrinoless decay mode occurs at all.

The early results on this Tellurium ratio, from the work of Hennecke et al. (Missouri group)[108] indicated some evidence for neutrinoless double beta decay. This result, however, has been contradicted by the recent publication of the Heidelberg group,[109] who find

$$\rho_T \equiv \frac{{}^{128}\lambda_T}{{}^{130}\lambda_T} = (1.03 \pm 1.13) \times 10^{-4} ,$$

i.e. no evidence for any enhancement due to neutrinoless decay mode. The implication of both of these results, in terms of limits (or values) of m_ν and η are shown in Fig. 46.

There is a program underway at UC Irvine to measure the double β decay process in ^{82}Se by measuring the energies of the 2 electrons resulting from the decay. The neutrinoless decay should exhibit itself as a spike in the total energy spectrum with a value corresponding to the total energy released. The early

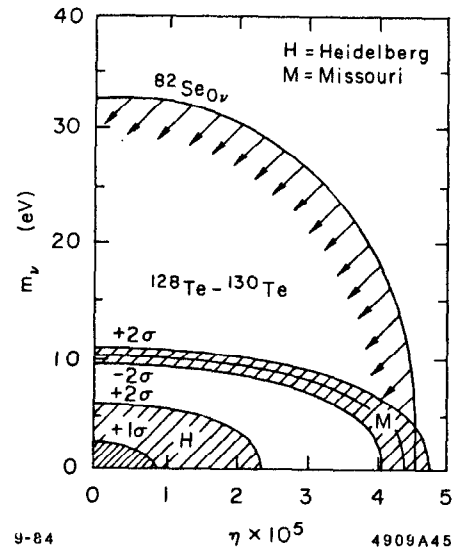

Figure 46 Allowed regions in the (m_ν, η) plane deduced from the measured ratios ρ_T of both the Heidelberg (H) and Missouri (M) analyses. The Se curve comes from the upper limit on $\lambda_{0\nu}$ from Cleveland et al., Phys. Rev. Lett. 35, 757 (1975).

experiment by Moe and Lowenthal[110] detected 20 clean $2e^-$ candidates using a cloud chamber, resulting in a half-life of $(1.0 \pm 0.4) \times 10^{19}$ years. This result was in significant disagreement with the previously accepted value, obtained by the geochemical means, of $(2.76 \pm 0.88) \times 10^{20}$ years, based on the analysis of the amount of selenium and krypton in tellurobismuthite.[111] The theoretical calculation for the 2ν rate[106] straddles these two experimental numbers with a value of 2.35×10^{19} years.

The UCI program is continuing, with a TPC detector scheduled to replace the previously used cloud chamber. If the cloud chamber result is correct, they should observe around 200 $2e^-$ events/month. A potential sensitivity to a no-ν partial lifetime of 2×10^{23} years is expected in two years of running.

A third general approach to the double β decay question involves attempts to observe $2e^-$ decays from ^{76}Ge using low background Ge detectors, generally located underground to reduce the cosmic ray background. There are at present 5 experiments in the preparation phase to perform this experiment. The *no* neutrino decay mode would exhibit itself as a line at 2.041 MeV and thus the goal of the experimenters is to reduce all the other backgrounds in this region as much as possible. The location and the preliminary background counting rates for those experiments as well as for the older Milano experiment are indicated below in Table VII.

Table VII

Preliminary Background Rates in Second Generation ^{76}Ge $\beta^-\beta^-$-Decay Experiments (given in counts/keV/hr/cm^3)

Experiment	Background at 2.041 MeV count/keV/hr/cm^3	Location
Milano (1983)	$\sim 1.6 \times 10^{-5}$	Mont Blanc Tunnel
Guelph-APTEC (1983)	$\sim 3.2 \times 10^{-5}$	Windsor Salt Mine
Battelle-Carolina (1983)	$\sim 2 \times 10^{-5}$	Battelle, above ground
Milano (1973)	$\sim 6.2 \times 10^{-5}$	Mont Blanc Tunnel
Battelle-Carolina (1982)	$\sim 6.2 \times 10^{-5}$	Battelle, above ground
Cal. Tech. (1983)	$\sim 2 \times 10^{-5}$	Pasadena, above ground

The ultimate sensitivity of the Ge experiments, assuming a running period of 4 years, is estimated to be about 10^{25} years. If this value is indeed achieved, it would correspond to[112]

$$m_\nu \leq 0.5 \text{ eV and } |\eta| < 10^{-6} .$$

This is probably the ultimate limit on the achievable neutrinoless double β decay sensitivity since the Ge detector combines very good energy resolution, good γ-ray background rejection, and favorable matrix element for this process. The present limits from all the studied doubled β decay sources are summarized[112] in Table VIII.

Table VIII

Present limits on $< m^{\mathrm{Maj}} >_\nu$ and $|\eta|$ from double beta decay experiments

Parent Isotope	$< m^{\mathrm{Maj}} >_\nu$	$\eta \times 10^5$	$< m^{\mathrm{Maj}} >_\nu^*$	$\eta \times 10^{5*}$
^{82}Se	$\leq$ 14 ev	$\leq$ 2	$\leq$ 33 eV	$\leq$ 4.6
^{130}Te	$\leq$ 8 eV	$\leq$ 2.3	$\leq$ 100 eV	$\leq$ 15
^{128}Te	$\leq$ 0.7 eV	$\leq$ 0.3	$\leq$ 8.7 eV	$\leq$ 3.5
^{48}Ca	$\leq$ 41 eV	$\leq$ 3.9	$\leq$ 44 eV	$\leq$ 4.2
^{76}Ge	$\leq$ 10 eV	$\leq$ 2.4	$\leq$ 24 eV	$\leq$ 4.5

*Values were analyzed with matrix elements renormalized to be in agreement with geochronological results in ^{130}Te and ^{82}Se. There is no compelling reason to do this.

6. RIGHT-HANDED CURRENTS

The original motivation for the right-handed currents rests in the explicit restoration of the right-left symmetry at the Lagrangian level. In this picture, we witness an asymmetry, i.e. predominantly a left-handed world, because we are in the low energy domain where this symmetry is broken. Explicitly, this is accomplished because $M_{W_R} >> M_{W_L}$ and as long as we are in the energy domain where $q^2 << M_{W_L}{}^2$, the observable weak interaction effects are due mainly to W_L. This framework might provide a natural mechanism of CP violation that is additional to that due to the presence of a phase in the Kobayashi-Maskawa matrix. That is accomplished by having a phase difference between W_L and W_R interactions. In this discussion, we shall limit ourselves strictly to the information that experiments provide about the question of the existence of the right-handed currents.

We shall compare the experimental situation with the classical model of right-left symmetry due to Bég, Budny, Mopatra, and Sirlin.[113] In that picture we have two states of well defined chirality W_R and W_L that mix to give mass eigenstates, W_1 and W_2 ,

$$W_1 = W_L \cos \varsigma - W_R \sin \varsigma, \text{and} \tag{6.1}$$

$$W_2 = W_L \sin \varsigma + W_R \cos \varsigma \ . \tag{6.2}$$

Thus data can be parametrized in terms of the mixing angle ς and the mass ratio squared α , defined by $\alpha = M^2(W_L)/M^2(W_R)$. Note that the α parameter is identical to the parameter η that is conventionally used in discussing the double β decay experiments.

We have already discussed the double β decay experiments and the relevance that they have on this question of R-L symmetry. One might only add here the caveat that all the conclusions drawn from these data rest on the assumption that we are dealing with a Majorana neutrino.

The first experiment that we shall discuss is the study of the endpoint of the electron energy spectrum from a muon decay in a direction opposite to the muon spin.[77] The results of that experiment are illustrated in Fig. 47. When the spin is precessed, the experiment effectively integrates over all the directions with respect to the spin and we are merely measuring the Michel ρ parameter (or alternatively detection efficiency, resolution, etc). This is illustrated in curve (A). When the spin is held, we see the rapid drop-off to the zero yield at the endpoint, as is predicted by the V-A theory. Quantitatively, the result can be expressed as a lower limit on the product of μ decay parameters and muon polarization and is $\xi P_\mu \delta/\rho > 0.9959$(90% C.L.). This value should be unity for pure V-A interaction.

The authors summarize[77] the results of their experiment as well as those of other low energy experiments that have a bearing on the question of right-handed currents. They are displayed as allowed contours in the $\varsigma - \alpha$ plane in Fig. 48. It should be emphasized that all of these results, with the exception of

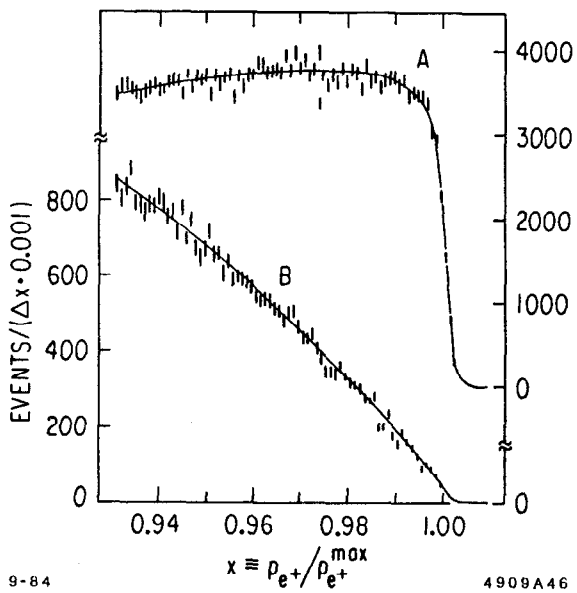

Figure 47 Distribution of the reduced positron momentum in the direction 180° away from the initial μ spin. Curve A is for the data taken with μ processing; curve B for μ spin held along the initial polarization direction.

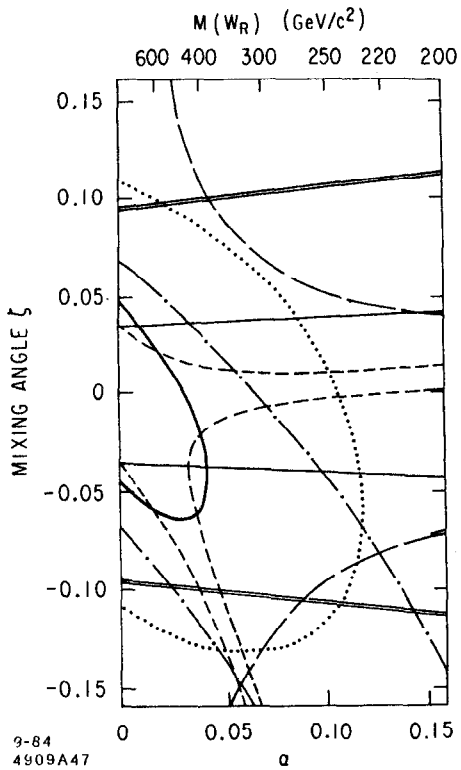

Figure 48 Experimental 90% -confidence limits on the W_L/W_R mass-squared ratio α and mixing angle ζ describing possible right-handed charged currents. The allowed regions are those which include $\alpha = \zeta = 0$. Muon-decay contours are derived from decay-rate measurements at the spectrum endpoint (bold curve), the polarization parameter ξP_μ (dotted curve) and the Michel parameter ρ (solid curve). Nuclear β-decay contours are obtained from the Gamow-Teller β polarization (dot-dashed curves); the comparison of Gamow-Teller and Fermi β polarizations (long-dashed curves); and the ^{19}Ne asymmetry A(0) and ft ratio, with the assumption of conserved vector current (short-dashed curves). Limits from the y distributions in νN and $\bar{\nu}$N scattering are shown as double lines.

the ν experiment to be discussed later, assume in their derivation of limits that $m_{\nu_R} \approx 0$.

A recent experiment at KEK[114] searched for the presence of right-handed currents in the decay $K^+ \rightarrow \mu^+\nu$. In principle, the expectation for this process could be independent of the μ decay experiment if the quark mixing angles are different in the right- and left-handed sectors. The specific experimental measurement is the polarization of the muon, predicted to be -1 in the V-A theory. The experimental value, $P_\mu = -0.970 \pm 0.047$ is fully compatible with that hypothesis.

The cross section for the reaction

$$\nu_\mu + e^- \rightarrow \mu^- + \nu_e$$

is sensitive to the handedness of the neutrinos and the nature of the charged leptonic current.[115] The experimental results are in perfect agreement[116] with the left-handed neutrinos and a V-A nature of the current.

The CDHS collaboration has searched[117] for possible admixtures of right-handed currents in the ν interactions. Experimentally these would show up as a deviation in the y distribution that one expects in a standard V-A picture. Thus, in the V-A picture the expected distribution for the ν scattering is

$$\frac{d^2\sigma^\nu}{dxdy} \;\alpha\; q(x) + (1-y)^2\bar{q}(x) \; .$$

If the Lagrangian has a right-handed contribution such as

$$L = \frac{G}{\sqrt{2}}\{\bar{\mu}\gamma_\mu(1+\gamma_5)\nu \times \bar{u}\gamma_\mu[C_L(1+\gamma_5) + C_R(1-\gamma_5)]d\}$$

then the differential distribution will be modified to

$$\frac{d^2\sigma^\nu}{dxdy} \;\alpha\; q(x) + \rho^2\bar{q}(x) + (1-y)^2[\bar{q}(x) + \rho^2 q(x)] \equiv q_L(x) + (1-y)^2 q_R(x)$$

where we have defined

$$\rho \equiv |C_R/C_L| \; .$$

For $\bar{\nu}$'s, we interchange the $q(x)$ and $\bar{q}(x)$ contributions (and $q_L(x)$ and $q_R(x)$).

Quantitatively, one compares the ratio of $\bar{\nu}$ to ν cross sections as a function of y and x (Fig. 49). Since this ratio vanishes at high x as $y \rightarrow 1$, we must have $q_R(x) << q_L(x)$. An upper limit on ρ^2 can be obtained by assuming that $\bar{q}(x) = 0$ in that limit, yielding a value of $|\rho^2| < 0.009$ with a 90 % confidence limit.

To relate this limit to our two standard parameters, we present in Fig. 50 the contribution of the right-handed currents to the neutrino quark scattering process. We assume that we have a pure beam of left-handed neutrinos and thus right-handed interaction occurs at the lower vertex by virtue of the mixing of W_L, or W_R, expressed previously in Eq. 6.1. Thus we have

$$C_R = \sin\,\varsigma\,\cos\,\varsigma\left(\frac{1}{M_{W_R}{}^2} - \frac{1}{M_{W_L}{}^2}\right) .$$

The left-handed interaction contribution has similar diagrams in this picture except that the coupling at the 2 vertices is either $\cos\,\varsigma$ or $\sin\,\varsigma$ depending on whether M_1 or M_2 is exchanged. We thus have

$$C_L = \frac{\cos^2\varsigma}{M_{W_L}{}^2} + \frac{\sin^2\varsigma}{M_{W_R}{}^2} \; .$$

For small values of the mixing angle we obtain

$$\varsigma \approx \rho/(1 - M_{W_L}{}^2/M_{W_R}{}^2) = \rho/(1-\alpha^2) \; .$$

Thus the experiment is mainly sensitive to the mixing angle; this fact is apparent from Fig. 48.

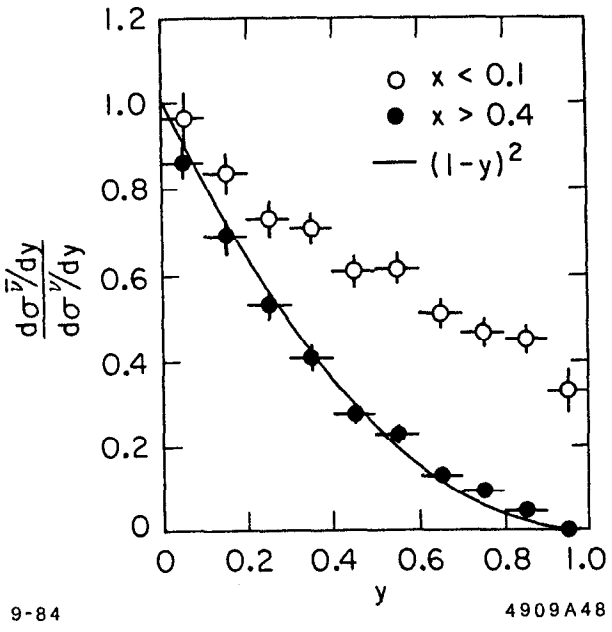

Figure 49 The ratio of antineutrino to neutrino cross sections as a function of y in two different regions of x.

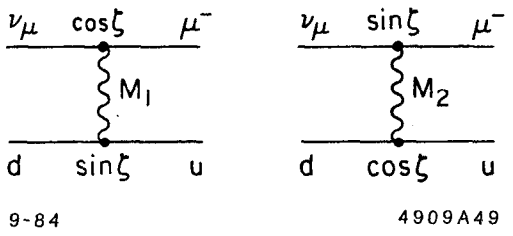

Figure 50 The 2 diagrams contributing to the right-handed interaction at the quark vertex if a left-handed neutrino initiates the reaction.

The CDHS Collaboration has also been able to explore[19] any possible contribution of the right-handed currents to interactions involving charm quarks, by studying the $\mu^+\mu^-$ channel that has been discussed previously in Chapter 2. Since that reaction has to proceed entirely off the quarks for incident neutrinos (and off the anti-quarks for incident $\bar{\nu}$'s), the right-handed currents are the sole possible contributor to the $(1-y)^2$ component for ν interactions (and to the isotropic component for $\bar{\nu}$'s). One can thus compare the Monte Carlo predictions for both the V-A and V+A predictions. Comparisons at 2 different energies are illustrated in Fig. 51. Clearly the data do not demand any V+A contribution and a quantitative analysis yields a 95% confidence limit on ρ^2 of $\rho^2 < 0.07$.

Finally, we might end this chapter by illustrating the sensitivity of a potential new high energy e^-p collider to right-handed currents. The cross sections[118] for the process $e^-p \to \nu_R + X$ are illustrated in Fig. 52. The projected rate of 1000 events/year assumes 10^7 secs of good running time. Thus even with these high energies the increase in M_{W_R} sensitivity is rather negligible over the lower energy experiments. It is important, however, to emphasize that these investigations would be independent of the mass of ν_R , provided only that $M_{\nu_R} << E_{cm}$.

Acknowledgements. I would like to thank L. Littenberg, M. Shaevitz, and B. Winstein for sending me copies of recent preprints and conference presentations that facilitated the preparation of these lectures.

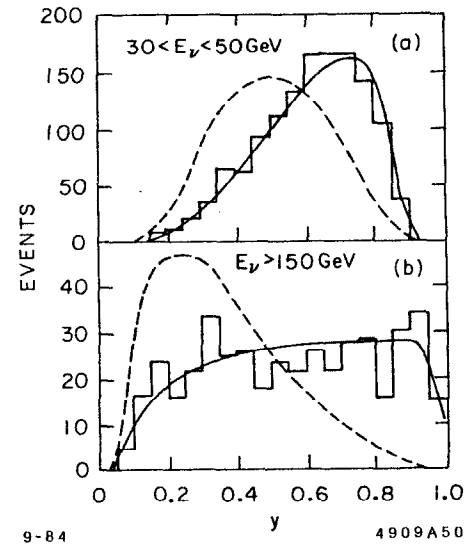

Figure 51 The y distribution of the observed $\mu^+\mu^-$ neutrino induced events for 2 different ranges of E_ν. The solid and dashed curves represent the V-A and V+A current predictions, respectively.

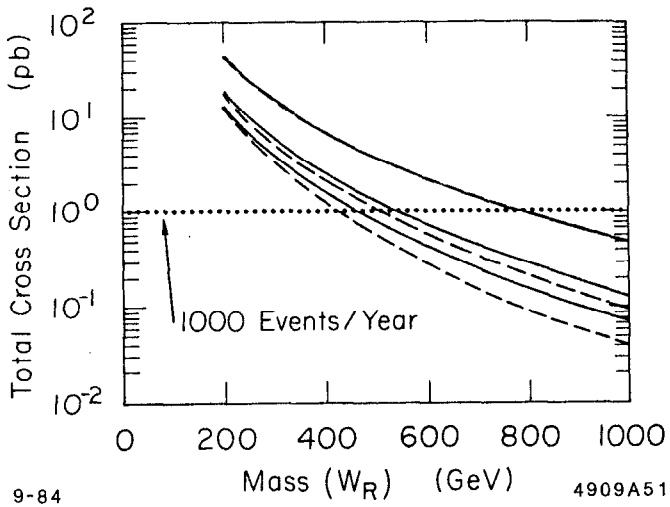

Figure 52 Cross section for the process $e^- p \to \nu_R + X$ computed in the limit $m_{\nu_R}, m_Q << E_{cms}$. (Q is the quark that emits or absorbs W_R.) The three sets of curves refer to electrons of energy 15 GeV, 30 GeV, and 200 GeV colliding with 20 TeV protons. The solid and dashed curves include angle cuts $\theta > 2°$ and $\theta > 10°$, respectively, on the produced fermions.

REFERENCES

1. It would be impossible for me to give appropriate credit to all the important experimental and theoretical work that contributed to the development of the subject under discussion. Accordingly I choose to avoid giving any references in this introductory chapter.
2. M. Kobayashi and K. Maskawa, Progr. Theor. Phys. 49, 652 (1973).
3. L. Maiani, **Proceedings of the 8th International Symposium on Lepton and Photon Interactions at High Energies**, Hamburg (1977), p. 867.
4. L. Wolfenstein, Phys. Rev. Lett. 51, 1945 (1983).
5. C. Rubbia, Recent Results from UA1 Experiment at CERN $\bar{p}p$ Collider, talk given at the Topical Conference at this Institute.
6. G. Kane and M. Peskin, Nucl. Phys. B195, 29 (1982).
7. S. Weinberg, Phys. Rev. Lett. 19 (1967) 1364; A. Salam, **Proc. 8th Nobel Symp.** (Almquist and Wiksells, Stockholm, 1968); S. Glashow, Nucl. Phys. 22, 579 (1961).
8. S. L. Glashow and S. Weinberg, Phys. Rev. D15 (1977) 1958.
9. CLEO Collaboration, paper C271 submitted to the 1983 International Symposium on Lepton and Photon Interactions at High Energies at Cornell; quoted by S. Stone, p. 217 of those Proceedings.
10. There have been several recent discussions of this question in the literature. The latest published work is probably by K. Kleinknecht and B. Renk, Phys. Lett. 130B (1983) 459.
11. E. A. Paschos and U. Turke, Phys. Lett. 116B 360 (1982).
12. R. E. Shrock and L. L. Wang, Phys. Rev. Lett. 41, 1962 (1978).
13. I. S. Towner and S. C. Hardy, Phys. Lett. 73B, 20 (1978); D. H. Wilkinson, Phys. Lett. 67B, 13 (1977).

14. M. Ademollo and R. Gatto, Phys. Rev. Lett. 13, 264 (1964).

15. M. Bourquin et al., Z. Phys. C21, (1983) 27.

16. Precision Measurement of the Decay $\Sigma^- \to ne^-\nu$, Fermilab Proposal No. 715, P. S. Cooper (Yale), spokesman.

17. R. H. Schindler et al., Phys. Rev. D24, 78 (1981).

18. D. Hitlin, Current Status of D Decays, talk given at the Topical Conference part of this Institute.

19. H. Abramowicz et al., Z. Phys. C15 (1982) 19.

20. Quoted by T. Nash in the **Proceedings of the 1983 International Symposium on Lepton and Photon Interactions at High Energies**, at Cornell, p. 359.

21. Heavy Hadron Decays, rapporteur talk by K. Schubert at the ν84 Conference in Dortmund.

22. S. Ahlen et al., Phys. Rev. Lett. 51, 1147 (1983).

23. W. Bacino et al., Phys. Rev. Lett. 43, 1073 (1979).

24. S. Pakvasa, S. F. Tuan, J. J. Sakurai, Phys. Rev. D23, 2799 (1981).

25. J. G. H. De Groot et al., Z. Phys. C1 (1979) 143.

26. K. Kleinknecht and B. Renk, Z. Phys. C16 (1982) 7.

27. C. Klopfenstein et al., Phys. Lett. 130B, 444 (1983).

28. A. Chen et al., Phys. Rev. Lett. 52, 1084 (1984).

29. M. K. Gaillard and L. Maiani, **Proc. Summ. Inst. on Quarks and Leptons, Cargese 1979** (Plenum, New York, 1980), p. 433.

30. E. Fernandez et al., Phys. Rev. Lett. 51, 1022 (1983); N. S. Lockyer et al., Phys. Rev. Lett. 51, 1316 (1983).

31. J. Jaros, Measurements of Heavy Quark and Lepton Lifetime at PEP, talk presented at the Topical Conference of this Institute.

32. D. E. Klem et al., submitted to Phys. Rev. Lett., SLAC-PUB-3379.

33. M. Davier, Recent Results from PETRA, talk presented at the Topical Conference at this Institute.

34. For a review of possible toponium decay modes, see J. D. Jackson, S. Olsen and S.-H. Tye, **Proceedings of the 1982 DPF Summer Study at Snowmass**, Colo., June 28 - July 16, 1982, p. 175.

35. L.-L. Chau and W.-Y. Keung, Phys. Rev. D29, 592 (1984).

36. L. Wolfenstein, Nucl. Phys. B160, 501 (1979).

37. J. Ellis, M. K. Gaillard, and D. V. Nanopoulos, Nucl. Phys. B109, 213 (1976).

38. P. H. Ginsparg, S. L. Glashow, and M. B. Wise, Phys. Rev. Lett. 50, 1415 (1983).

39. R. E. Shrock and S. B. Treiman, Phys. Rev. D19, 2148 (1979).

40. M. K. Gaillard and B. W. Lee, Phys. Rev. D10, 897 (1974).

41. J. F. Donoghue et al., Phys. Lett. 119B, 412 (1982).

42. See for example A. Buras, Phys. Rev. Lett. 46, 1354 (1980).

43. J. H. Christenson et al., Phys. Rev. Lett. 13, 138, (1964).

44. For a recent comprehensive review, see K. K. Kleinknecht, Ann. Rev. Nucl. Science 26, 1 (1976).

45. F. J. Gilman and M. Wise, Phys. Rev. D20, 2392 (1979); B. Guberina and R. D. Peccei, Nucl. Phys. B163, 289 (1980).

46. L. Wolfenstein, Phys. Rev. Lett. 13, 562 (1964).

47. F. J. Gilman and J. S. Hagelin, Phys. Lett. 133B, 443 (1983) and Phys. Lett. 126B, 111 (1983). See also Ref. 45.

48. B. Winstein, review talk given at the XIth International Conference on Neutrino Physics and Astrophysics at Dortmund, June 11-16, 1984.

49. J. Cronin, CP Violation in K Decays, talk given at the Topical Conference part of this Institute.

50. W. M. Morse, Measurement of ϵ' at the AGS, talk given at the 1984 Conference in Erice, Sicily, Italy.

51. A measurement of the magnitude of ϵ'/ϵ in the neutral Kaon system to a precision of 0.001, Fermilab Proposal E-731, Chicago, Fermilab, Saclay collaboration; B. Winstein, Chicago, spokesman.

52. Measurement of $|\eta_{oo}|^2/|\eta_{+-}|^2$, CERN/SPSC/81-110 , December 22, 1981; proposal to CERN SPS; H. Wahl, CERN, spokesman.

53. M. K. Campbell et al., Phys. Rev. Lett. 47, 1032 (1981).

54. W. M. Morse et al., Phys. Rev. D21, 1750 (1980).

55. Letter of intent by Backenstoss et al., CERN/PSCC/83-28; PSCC/I 65, June 9, 1983.

56. Fermilab proposal # 621; Wisconsin, Rutgers, Michigan, Minnesota collaboration; G. Thomson, U. of Wisconsin, spokesman.

57. Study of very rare K_L° decays, AGS proposal # 791 by UCLA-Los Alamos, Pennsylvania, Princeton, Stanford, Temple, William and Mary collaboration; S. Wojcicki, Stanford, spokesman.

58. F. J. Gilman and M. B. Wise, Phys. Rev. D21, 21 (1980).

59. P. Herczeg, Phys. Rev. D27, 1512 (1983).

60. L.-L. Chau, W.-Y. Keung, M. D. Tran, Phys. Rev. D27, 2145 (1983).

61. W. B. Dress et al., Phys. Rev. D15, 9 (1979).

62. D. V. Nanopoulos, A. Yildiz, and P. H. Cox, Phys. Lett. B87, 53 (1979); B. F. Morel, Nucl. Phys. B157, 23 (1979).

63. I. I. Bigi and A. I. Sanda, Nucl. Phys. B193, 85 (1981).

64. A. Bodek et al., Phys. Lett. 113B, 82 (1982).

65. I. I. Bigi and A. I. Sanda, Phys. Rev. D29, 1393 (1984).

66. J. S. Hagelin, Nucl. Phys. B193, 123 (1981).

67. R. N. Cahn and H. Harari, Nucl. Phys. B176, 135 (1980).

68. J. Ellis and J. S. Hagelin, Nucl. Phys. B217, 189 (1983).

69. F. Wilczek, Phys. Rev. Lett. 49, 1549 (1982).

70. A Study of the Decay $K^+ \to \pi^+\nu\bar{\nu}$, AGS Experiment # 787, BNL, Carnegie Mellon, Columbia, Princeton, TRIUMF Collaboration.

71. Y. Asano et al., Phys. Lett. 107B, 159 (1981).

72. A Search for the Rare Decay $K^+ \to \pi^+\mu^+e^-$, AGS experiment # 777, a Brookhaven, Washington, Yale collaboration; M. Zeller, Yale, spokesman.

73. A. M. Diamant-Berger et al., Phys. Lett. 62B, 485 (1976).

74. A Search for the Flavor Changing Neutral Currents $K_L^\circ \to \mu + e$ and $K_L^\circ \to e^+e^-$, AGS experiment # 780, BNL-Yale Collaboration, M. P. Schmidt (Yale) and W. M. Morse (BNL), spokesmen.

75. G. J. Feldman, in the **Proceedings of the 1981 DPF Annual Meeting**, Santa Cruz, Ca., C. A. Heusch and W. T. Kirk, ed; also K. G. Hayes et al., Phys. Rev. D25, 2869 (1982).

76. F. Scheck, Phys. Rep. C44, 187 (1978).

77. J. Carr et al., Phys. Rev. Lett. 51, 627 (1983).

78. W. Bacino et al., Phys. Rev. Lett. 42, 749 (1979).

79. J. A. Jaros et al., Phys. Rev. Lett. 51, 955 (1983).

80. For example see A. DeRujula et al., Nucl. Phys. B168, 54 (1980).

81. K. E. Berquist, Phys. Scripta 4, 23 (1971) and Nucl. Phys. B39, 317 (1972).

82. V. A. Lubimov et al., Phys. Lett. 94B, 266 (1980).

83. V. A. Lubimov, **Proceedings of the European Physical Society HEP 83**, Brighton, England; see also the review talk by M. Shaevitz, in the **Proceedings of the 1983 International Symposium on Lepton and Photon Interactions at High Energies**, Cornell, N.Y.

84. See the review paper by F. Boehm in the **Proceedings of the 4th Workshop on Grand Unification**, Birkhäuser Boston, p. 163, (1983).

85. A. DeRujula, Nucl. Phys. B188, 414 (1981).

86. J. U. Anderson et al., Phys. Lett. 113B, 72 (1982).

87. R. S. Raghaven, Phys. Rev. Lett. 51, 975 (1983).

88. R. Abela et al., Phys. Lett. 105B, 263 (1981).

89. C. Matteuzzi et al., Phys. Rev. Lett. 52, 1869 (1984).

90. R. Schrock, Phys. Lett. 96B, 159 (1980).

91. K. Winter, in **Proceedings of the 1983 International Symposium on Lepton and Photon Interactions at High Energies**, Cornell, N.Y., p. 177.

92. D. Silverman and A. Soni, **Proceedings of the Annual DPF Conference**, at Santa Cruz, 1981.

93. See for example J. N. Bahcall, R. Davis, Science 191, 264 (1976).

94. J. N. Bahcall et al., Rev. Mod. Phys. 54, 767 (1982).

95. R. Davis et al., **Proceedings of the International Neutrino Conference**, Purdue Ill., 1978, p. 53; W. Hampel, **Proceedings of the International Conference on Neutrino Physics and Astrophysics**, Erice, 1980, p. 61.

96. M. R. Krishnaswamy et al., **Proc. Roy. Soc. London A323**, 489 (1971); M. F. Crouch et al., Phys. Rev. D18, 2239 (1978).

97. M. M. Bolieu et al., **Proc. 1981 Intern. Conf. on Neutrino Phys. and Astroph.**, Maui, 1981, vol. I, p. 283; G. D. Davimus, ibid. p. 291.

98. R. M. Bionta et al., **Proceedings of the 4th Workshop on Grand Unification**, Birkhäuser: Boston, p. 46, 1983.

99. T. Gaisser, ibid., p. 87.

100. See for example I. E. Stockdale et al., Phys. Rev. Lett. 52, 1384 (1984); F. Bergsma, Phys. Lett. 142, 103 (1984); F. Dydak et al., Phys. Lett. 134B, 281 (1984).

101. F. Reines et al., Phys. Rev. Lett. 45, 1307 (1980); F. Boehm et al., Phys. Lett. 97B, 310 (1980). The Irvine experiment compared charged current and neutral current reactions, the latter being insensitive to any ν_e depletion due to oscillations.

102. H. Kwon et al., Phys. Rev. D24, 1097 (1981).

103. J. L. Vuillemier et al., Phys. Lett. 114B, 298 (1982).

104. J. L. Vuillemier, paper presented at the XIth International Conference on Neutrino Physics and Astrophysics at Dortmund, June 11-16, 1984.

105. D. Koang, paper presented at the XIth International Conference on Neutrino Physics and Astrophysics at Dortmund, June 11-16, 1984.

106. See for example W. C. Haxton, G. J. Stephenson, Jr., and D. Strottman, Phys. Rev. Lett. 47, 153 (1981).

107. B. Pontecorvo, Phys. Lett. 26B, 630 (1968).

108. E. Hennecke et al., Phys. Rev. C11, 1378 (1975).

109. T. Kirsten, H. Richter and E. Jessberger, Phys. Rev. Lett. 50, 474 (1983).

110. M. K. Moe and D. D. Lowenthal, Phys. Rev. C22, 2186 (1980).

111. B. Srinivasan et al., Econ. Geol. 68, 252 (1973).

112. F. T. Avignone, III et al., review talk given at the Fourth Workshop on Grand Unification, Philadelphia, Pa., April 21-23, Birkhaüser-Boston, publishers.

113. M. A. B. Bég et al., Phys. Rev. Lett. 38, 1252 (1977).

114. R. S. Hayano et al., Phys. Rev. Lett. 52, 329 (1984).

115. C. Jarlskog, Nuov. Cim. Lett. 4, 377 (1970).

116. N. Armenise et al., Phys. Lett. 84B, 137 (1979); M. Jonker et al., Phys. Lett. 93B, 203 (1980).

117. H. Abramowicz et al., Z. Phys. C12, 225 (1982).

118. C. Prescott, in the Summary Report of the PSSC Discussion Group Meetings, P. Hale and B. Winstein, editors.